10-5-2017

The Variational Calculation of the 413 nm 4He Tune-out Wavelength

Jacob Manalo
University of Windsor

The Variational Calculation of the 413 nm ^{4}He Tune-out Wavelength

by

Jacob G. Manalo

A Thesis
Submitted to the Faculty of Graduate Studies
through the Department of Physics in Partial Fulfillment
of the Requirements for the Degree of Master of Science at the
University of Windsor

Windsor, Ontario, Canada
2017

The Variational Calculation of the 413 nm ^{4}He Tune-out Wavelength

by

Jacob G. Manalo

APPROVED BY:

J. W. Gauld
Department of Chemistry and Biochemistry

W. Kedzierski
Department of Physics

G. W. F. Drake, Advisor
Department of Physics

August 31, 2017

Author's Declaration of Originality

I hereby certify that I am the sole author of this thesis and that no part of this thesis has been published or submitted for publication.

I certify that, to the best of my knowledge, my thesis does not infringe upon anyones copyright nor violate any proprietary rights and that any ideas, techniques, quotations, or any other material from the work of other people included in my thesis, published or otherwise, are fully acknowledged in accordance with the standard referencing practices. Furthermore, to the extent that I have included copyrighted material that surpasses the bounds of fair dealing within the meaning of the Canada Copyright Act, I certify that I have obtained a written permission from the copyright owner(s) to include such material(s) in my thesis and have included copies of such copyright clearances to my appendix.

I declare that this is a true copy of my thesis, including any final revisions, as approved by my thesis committee and the Graduate Studies office, and that this thesis has not been submitted for a higher degree to any other University or Institution.

Abstract

A tune-out wavelength of an atom is a wavelength of radiation such that the atom's polarizability vanishes [1]. It can be used as an alternative to inducing energy shifts for the purpose of testing quantum electrodynamics (QED). This is done by incorporating perturbations to the polarizability and calculating a chosen root, i.e. a tune-out wavelength. Comparison with experiment can determine the effectiveness of the theory from which these perturbations arise. In this study, the calculated 2^3S - 3^3P transition tune-out wavelength for ^{4}He was compared with an interferometry experiment done by Kenneth Baldwin's group at the Australian National University. The calculated result of 413.0858252(4) nm, which takes into account fine-structure effects and other relativistic corrections of order $\frac{1}{c^2}$, differs from the experimental value of $413.0938(9_{\text{stat}})(20_{\text{syst}})$ nm [2] by about 1 part in 10, 000. This discrepancy is suspected to be due to QED effects such as the atom's interaction with the vacuum, which is why QED perturbations should be tested as well in the future. The calculation of the 2^3S - 3^3P transition tune-out wavelength basically served as an exercise in studying the perturbative effects of relativity to the order of $\frac{1}{c^2}$.

To my parents Josefina and Josefino Manalo, and to my dear friend Kyle, who has agreed to call me a Master upon completion of my degree.

See you soon, brother!

Acknowledgements

I would like to thank Gordon Drake for giving me the opportunity to pursue a Masters under him and for helping me hone my intuition in physics, something that is still a work in progress today.

I would also like to thank my colleagues Eva Schulhoff, Maha Sami, Ryan Peck, Daniel Venn and Spencer Percy for their academic support and also for contributing to a warm and inviting environment that I will never forget.

Finally, I would like to thank my family, namely my parents Josefino and Josefina Manalo for their encouragement, my aunt Corazon Tayag, my cousin Christel Tayag and her beloved children Ivanka and Sebastian for making Windsor feel like a second home to me.

Table of Contents

List of Figures

List of Tables

Chapter 1

Introduction

When an atom is in an electromagnetic field, the charges redistribute and a dipole moment forms. The quantity that describes the degree to which this dipole is polarized is known as the polarizability. If the field is oscillating i.e. if the field is an electromagnetic (EM) wave, then the polarizability of the atom becomes a function of the wavelength of the interacting EM wave. At certain wavelengths, the polarizability becomes zero. These wavelengths are called tune-out wavelengths and they are the field wavelengths such that they do not distort the atom [1].

The main reason for calculating and measuring tune-out wavelengths for ^{4}He is to test quantum electrodynamics (QED) which is the most fundamental physical theory describing all EM phenomena. One way of testing QED is to measure the Lamb shift, which is the energy shift of the $^2S_{\frac{1}{2}}$ - $2P_{\frac{1}{2}}$ transition for hydrogen [**?**]. Without incorporating QED, the energies of these two states are degenerate [5], which makes measuring the Lamb shift suitable for testing QED. A major contribution to this energy shift is the anomalous magnetic moment, which is a QED correction to the Dirac magnetic moment [**?**].

Using interferometric techniques as performed by Baldwin and his group at ANU, these wavelengths can be measured in order to test the validity of QED without in-

ducing energy shifts [2][6]. This new method of testing QED, which acts as a test for the off-diagonal matrix elements has never been done before.

The measurement and calculation of the tune-out wavelength of ^{4}He nearest to the 2 ^{3}S - 3 ^{3}P transition serves as the best test for QED involving tune-out wavelengths since this specific tune-out wavelength is most sensitive to dynamical effects [6]. This tune-out wavelength was measured to be $413.0938(9_{\text{stat}})(20_{\text{syst}})$ nm according to Baldwin's experiment [2].

The method of calculating the theoretical value of the 413 nm tune-out wavelength is to add relativistic perturbations, and eventually QED perturbations, to the nonrelativistic three-body Schrödinger Hamiltonian. Since the polarizability is zero at the tune-out wavelength, it is necessary to calculate the polarizability first, which by definition is the second order perturbation energy where the perturbation is an external field. Relativistic perturbations of the first order are then added to the polarizability. These corrections come from the relativistic kinetic energy, fine-structure splitting and relativistic finite nuclear mass effects. Once all of the perturbations are included, the root closest to the 2 ^{3}S - 3 ^{3}P transition, which is the 413 nm tune-out wavelength, is computed. The theoretical 413 nm tune-out wavelengths with all of the corrections to the order α^2 are 413.07995862(11) nm for the $m = 0$ substate 413.08582525(12) nm for the $m = \pm 1$ substates. These are currently the most accurate calculations for the 413 nm tune-out wavelength. The reason why the measured value does not distinguish between the different magnetic substates is because the difference between the two is experimentally negligible [2]. The current discrepancy of several femtometres between theory and experiment is of the same order of magnitude as what the QED corrections should be [7]. Now that the necessary foundation for the theoretical tune-out wavelength calculation has been formed, future perturbative calculations for the QED corrections can be made. If there is still a discrepancy between theory and experiment even after QED has been accounted for, then perhaps it could be accounted for by new physics, yet to be discovered.

Chapter 2

Solutions to the Three Body Problem

Before including any perturbations from the field and relativistic effects in the tune-out wavelength calculation, it is imperative to understand the solutions to the nonrelativistic three-body problem, upon which the perturbations from the field and relativity are built. There are two main approximations that are used for such solutions, which are the finite and infinite nuclear mass approximations. The finite mass approximation takes into account the motion of the nucleus relative to the centre-of-mass, and the infinite mass approximation is the Hamiltonian that arises from taking the infinite mass limit of the nucleus.

The solutions are computed by diagonalizing the Hamiltonian in a discrete variational basis set and the result is a set of pseudostate solutions.

2.1 Center of Mass Coordinates

The Hamiltonian for the three body problem is shown below

$$H = \frac{1}{2M}p_N^2 + \frac{1}{2m}(p_1^2 + p_2^2) - \frac{Ze^2}{r_1} - \frac{Ze^2}{r_2} + \frac{e^2}{r_{12}} \tag{2.1}$$

[8]

where the coordinates r_1 (the position of one electron), r_2 (the position of the other electron) and r_{12} (the distance between the two electrons) determine the geometry of the system. The potential consists of the Coulomb interaction between each electron and the nucleus and the interaction between the two electrons.

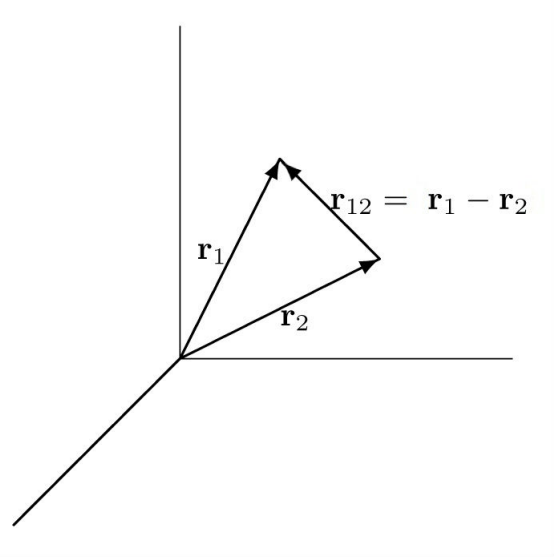

Figure 2.1: Diagram of Hylleraas Coordinates

To eliminate the centre-of-mass motion, the following substitutions are made to switch to centre-of-mass coordinates.

$$\vec{R} = \frac{1}{M+nm}\left[M\vec{r}_N + m(\vec{r}_1 + \vec{r}_2 + \ldots)\right] \tag{2.2}$$

$$\vec{s}_i = \vec{r}_i - \vec{r}_N \tag{2.3}$$

The following Hamiltonian becomes

$$H = \frac{1}{2\mu}(p_{s_1}^2 + p_{s_2}^2) + \frac{1}{2M}\vec{p}_{s_1} \cdot \vec{p}_{s_1} + V(s_1, s_2). \tag{2.4}$$

The change of coordinates introduces the $\vec{p}_1 \cdot \vec{p}_2$ term, known as the mass polarization term. This perturbation strictly comes from the nuclear mass being finite. In the limit as $M \to \infty$, the finite mass correction disappears. The infinite mass Hamiltonian is then

$$H = \frac{1}{2m}(p_1^2 + p_2^2) + V. \tag{2.5}$$

It then follows that $\vec{R} \to 0$ and $\vec{s_i} \to \vec{r_i}$ if the position of the nucleus $\vec{r_N}$ is taken to be the origin.

Now that the groundwork has been laid for the finite and infinite mass Hamiltonians, its solutions can be computed. Since the three body problem cannot be solved exactly, approximate solutions are obtained variationally by diagonalizing the Hamiltonian.

2.2 Linear Variational Method

The solutions to the three body Hamiltonian are obtained using the variational principle. A trial function

$$\Psi_{tr} = \sum_{i}^{N} c_i \phi_i$$

where the ϕ_i's form a complete basis set in the limit $N \to \infty$ is proposed.

Using this basis set, an expression for the expectation value of the ground state energy is obtained

$$\begin{aligned} E_{tr} &= \frac{\langle \Psi_{tr}|H|\Psi_{tr}\rangle}{\langle \Psi_{tr}|\Psi_{tr}\rangle} \\ &= \frac{\sum_{ij} c_i^* c_j \langle \phi_i|H|\phi_j\rangle}{\sum_{ij} c_i^* c_j \langle \phi_i|\phi_j\rangle} \end{aligned} \tag{2.6}$$

[9]

By employing the following minimization condition,

$$\frac{\partial E_{tr}}{\partial c_i} = 0 \tag{2.7}$$

we obtain the system of N equations

$$\sum_{i=1}^{N} (\langle \phi_i|H|\phi_k\rangle - E_{tr}\langle \phi_i|\phi_k\rangle) c_i = 0 \tag{2.8}$$

[9]

If Eq.(2.8) is re-expressed as the matrix equation,

$$\begin{bmatrix} \langle \phi_1|H|\phi_1\rangle & \dots & \langle \phi_1|H|\phi_N\rangle \\ \vdots & \ddots & \vdots \\ \langle \phi_N|H|\phi_1\rangle & \dots & \langle \phi_N|H|\phi_N\rangle \end{bmatrix} \begin{bmatrix} c_1 \\ \vdots \\ c_N \end{bmatrix} = E_{tr} \begin{bmatrix} \langle \phi_1|\phi_1\rangle & \dots & \langle \phi_1|\phi_N\rangle \\ \vdots & \ddots & \vdots \\ \langle \phi_N|\phi_1\rangle & \dots & \langle \phi_N|\phi_N\rangle \end{bmatrix} \begin{bmatrix} c_1 \\ \vdots \\ c_N \end{bmatrix} \tag{2.9}$$

then the minimization problem becomes equivalent to a generalized eigenvalue problem, whose solution yields N eigenvalues (E_1,...,E_N). The eigenvalues and eigenvectors are obtained by first diagonalizing the overlap matrix containing the $\langle\phi_i|\phi_j\rangle$ elements, and then diagonalizing the Hamiltonian. The set of basis functions ϕ_i can be any set of functions, provided the functions form a complete set. For our calculations, we use the Hylleraas basis functions

$$\phi_m = r_1^i r_2^j r_{12}^k e^{-\alpha r_1 - \beta r_2} \mathcal{Y}^M_{l_1,l_2,L}(\hat{r}_1, \hat{r}_2) \pm (r_1 \leftrightarrow r_2) \tag{2.10}$$

where the subscript m denotes the mth combination of i, j and k and $\mathcal{Y}^M_{l_1,l_2,L}(\hat{\mathbf{r}}_1, \hat{\mathbf{r}}_2) = \sum_{m_1,m_2} Y^{m_1}_{l_1}(\mathbf{r}_1) Y^{m_2}_{l_2}(\mathbf{r}_2) \times \langle l_1 l_2 m_1 m_2 \mid LM\rangle$ is a vector coupled spherical harmonic. The advantage of these functions is that the electron-electron coordinate r_{12} is built into them. These functions yield relatively fast convergence when calculating energy levels in comparison to alternative basis functions as discussed in Section 3.4.

2.3 Pseudospectrum Method

The trial energy from the previous section forms an upper bound to the true ground state energy. This is easily shown by substituting a normalized trial wave function into E_{tr}.

$$\begin{aligned} E_{tr} &= \langle\Psi_{tr}|H|\Psi_{tr}\rangle \\ &= c_0^2 E_0 + c_1^2 E_1 + C_2^2 E_2 + \dots \\ &= (1 - c_1^2 - c_2^2 + \dots) E_0 + c_1^2 E_1 + c_2^2 E_2 + \dots \\ &= E_0 + c_1^2 (E_1 - E_0) + c_2^2 (E_2 - E_0) + \dots \\ &\geq E_0 \end{aligned} \tag{2.11}$$

This concept can be extended to excited states using the Hylleraas-Unheim-MacDonald theorem [10]. According to this theorem, as an extra row and column is added to the Hamiltonian, the N old eigenvalues lie inbetween the $N+1$ new eigenvalues [3].

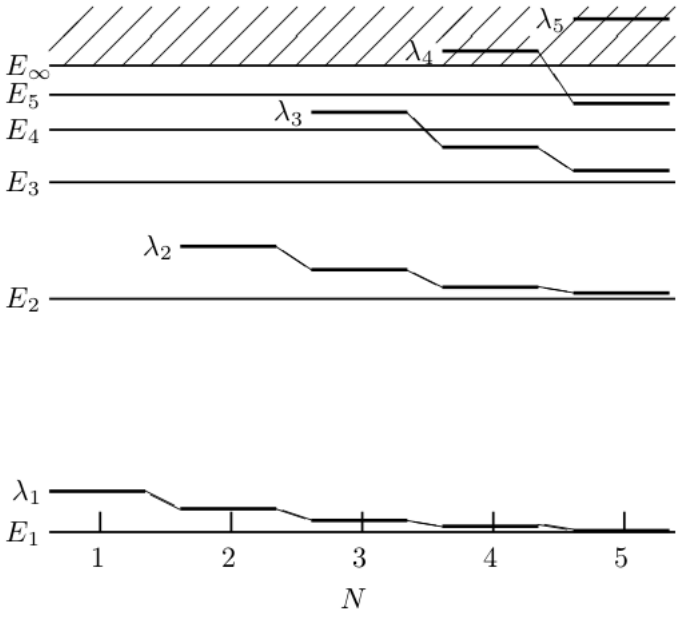

Figure 2.2: Illustration of the Hylleraas-Unheim-Macdonald theorem. The previous N eigenvalues lie between the new ones as N increases [3]

As N increases, the eigenvalues progressively move downward until they reach the exact physical energies as shown in Figure 2.2. Furthermore, some of the higher lying eigenvalues lie in the ionization continuum provided that N is large enough, thus representing a range of physical states that lie in the continuum. These pseudostates then form a discrete variational representation of the physical spectrum and is computationally advantageous over using the actual spectrum when being used to sum over intermediate states. This is because relatively few pseudostates are needed to represent a large portion of the physical spectrum. The example shown in Figure 2.2 shows that a five term basis set spans the physical bound states plus a portion of the continuum. In fact, the exact ground-state polarizability of hydrogen can be computed using only a two-term basis set, which is discussed in further detail in the next chapter.

Chapter 3

Polarizability

3.1 Static Polarizability

The static polarizability of an atom is a measure of how an atom distorts in an external electric field. It describes the degree to which it forms a dipole moment. Mathematically speaking, the polarizability is defined as the first order coefficient in the Taylor expansion of the dipole moment about the field strength. In quantum mechanics, this corresponds to the second order perturbation energy when the potential due to the external field acting on the electron is treated as a perturbation, as discussed in this section.

To begin, the Taylor expansion of the dipole moment as a function of field strength is

$$\mu = \alpha_{\alpha\beta} F_\beta + \frac{1}{2}\beta_{\alpha\beta\gamma} F_\beta F_\gamma + \dots \tag{3.1}$$

[11]

where the α, β and γ indices denote spatial response of the molecule to the field, similar to the indices of a stress tensor describing the deformation of a crystal in a field.

Assuming that the molecule is axially symmetric, the only terms in the dipole energy

$\vec{\mu} \cdot \vec{E}$ that survive are the ones with even powers of F according to

$$\vec{\mu} \cdot \vec{E} = -\frac{1}{2}\alpha F^2 - \frac{1}{24}\gamma F^4 - \dots \tag{3.2}$$

Now consider the Hamiltonian with a perturbation from the external field.

$$H = H_0 - eFz \tag{3.3}$$

By comparing the powers of F in the perturbation energy shift with those in the dipole energy expansion, it is clear that the second order perturbed energy corresponds to the polarizability. This is where the quantum definition of the polarizability comes from Eq.(3.5). Again, the odd powers vanish due to the parity of the dipole operator z.

$$\Delta E = E^2 F^2 + E^4 F^4 \tag{3.4}$$

$$E^2 = -\frac{1}{2}\alpha \tag{3.5}$$

Finally, an expression for the static polarizability is obtained from the second order perturbation equation, using the facts that $E^1 = \langle \Psi^0 | V | \Psi^0 \rangle = 0$ and that the perturbed states form an orthonormal basis set.

$$\langle \psi^0 | (H_0 - E_0) | \psi^2 \rangle = \langle \psi^0 | (ez|\psi^1\rangle + E^2|\psi^0\rangle + E^1|\psi^1\rangle) \tag{3.6}$$

$$\rightarrow E^2 = e\langle \psi^0 | z | \psi^1 \rangle \tag{3.7}$$

$$\rightarrow \alpha = -2e\langle \psi^0 | z | \psi^1 \rangle \tag{3.8}$$

This expression (3.8) will be used in the next section to obtain the dynamic polarizability, which describes a the response of a molecule to an oscillating field. The zero frequency limit of this dynamic polarizability is the static polarizability.

3.2 Dynamic Polarizability

The dynamic polarizability of an atom is a measure of how the atom responds to an oscillating EM field. This situation can be modelled with a Hamiltonian describing an atom in an oscillating electric field

$$H = H_0 - eFz\cos(\omega t) \tag{3.9}$$

where ω is the oscillation frequency and $z \equiv \sum_i z_i$.
To derive the dynamic polarizability, the cosine factor in the potential can be split into exponentials according to the definition of cosine.

$$\begin{aligned} V(z,t) &= -eFz\frac{e^{i\omega t} + e^{-i\omega t}}{2} \\ &\equiv F[G_+(z,t) + G_-(z,t)] \end{aligned} \tag{3.10}$$

Substituting the new expression for V in the Schrödinger equation gives

$$i\hbar\frac{\partial}{\partial t}|\Psi(t)\rangle = (H_0 + FG_+ + FG_-)|\Psi(t)\rangle. \tag{3.11}$$

From here, G can be treated as a perturbation in order to expand the wave function

$$|\Psi(t)\rangle = |\psi^0(t)\rangle + F(|\psi^1_+(t)\rangle + |\psi^1_-(t)\rangle) + ... \tag{3.12}$$

The wave function is then substituted back into the Schödinger equation in order to obtain the zeroth (3.13) and first (3.14) order perturbation equations

$$(H_0 - i\hbar\frac{\partial}{\partial t})|\psi^0(t)\rangle = 0 \tag{3.13}$$

$$(H_0 - i\hbar\frac{\partial}{\partial t})|\psi^1_\pm(t)\rangle = G_\pm|\psi^0(t)\rangle \tag{3.14}$$

In order to obtain steady-state solutions, it must be assumed that the field was

switched on adiabatically, so transient effects will have died away. If this assumption is made, the steady-state solutions take on the form

$$|\psi^0(t)\rangle = |\psi^0\rangle e^{iE_n t/\hbar} \tag{3.15}$$

$$|\psi^1(t)\rangle = |\psi^1_\pm\rangle e^{iE_n t/\hbar \pm i\omega t} \tag{3.16}$$

Substituting these solutions into the perturbation equations (3.13) and (3.14), the new 0th and 1st order equations become

$$(H_0 - E_0)|\psi^0\rangle = 0 \tag{3.17}$$

$$(H_0 - E_0 \pm \hbar\omega)|\psi^1_\pm\rangle = -\frac{1}{2} z|\psi^0\rangle. \tag{3.18}$$

Now for the final step of deriving the dynamic polarizability, Eq.(3.18) is substituted into Eq.(3.8) to obtain

$$\alpha(\omega) = e^2(\langle\psi^0|z\frac{1}{H_0 - E_0 + \hbar\omega}z|\psi^0\rangle + \langle\psi^0|z\frac{1}{H_0 - E_0 - \hbar\omega}z|\psi^0\rangle) \tag{3.19}$$

This is the expression for the nonrelativistic dynamic polarizability. For the purpose of calculation, a complete set of intermediate states is inserted in between the resolvent operators $(H_0 - E_0 \pm \hbar\omega)^{-1}$ and the dipole operator to obtain

$$\begin{aligned}
\alpha(\omega) =& \sum_i e^2\langle\psi^0|z\frac{1}{H_0 - E_0 + \hbar\omega}|i\rangle\langle i|z|\psi^0\rangle \\
&+ e^2\langle\psi^0|z\frac{1}{H_0 - E_0 - \hbar\omega}|i\rangle\langle i|z|\psi^0\rangle \\
=& \sum_i e^2\langle\psi^0|z|i\rangle^2(\frac{1}{E_0 - E_i + \hbar\omega} + \frac{1}{E_0 - E_i - \hbar\omega}) \\
=& 2e^2\sum_i \frac{(E_i - E_0)\langle\psi^0|z|\psi^i\rangle^2}{(E_i - E_0)^2 - (\hbar\omega)^2}
\end{aligned} \tag{3.20}$$

The sum over the intermediate states is traditionally carried out by summing over the bound states and integrating over the continuum. This is where the pseudospectral

method in the previous chapter comes in. Instead of inserting the actual spectrum, one inserts a discrete variational basis set. Computationally speaking, this basis set is obtained by first orthonormalizing a set of Hylleraas functions ϕ_p via a unitary transformation R such that $\Phi_m = \sum_n^N \phi_n R_{nm}$ and $\langle \Phi_m | \Phi_n \rangle = \delta_{mn}$. Once the basis functions have been orthonormalized, another unitary transformation W is applied to the Hamiltonian. The result is a pseudospectrum of states $\Psi^{(q)}$ where $\Psi^{(q)} = \sum_n^N \Phi_n W_{nq}$. This diagonalization method is discussed in further detail in the Appendix.

3.3 Application of Pseudospectral Method to Hydrogen

To demonstrate the power of the pseudospectral method, this section applies it to the simple case of hydrogen. Given the Hamiltonian of an atom in a static field

$$H = H_0 + eFr\cos\theta \tag{3.21}$$

a variational solution to the first-order perturbation equation consisting of Sturmian functions can be constructed according to

$$\phi_{tr} = -\frac{1}{\sqrt{(3)}}(b_1 r + b_2 r^2)e^{-\lambda r}Y_1^0(\cos\theta) \tag{3.22}$$

where $\chi_1 = -\frac{1}{\sqrt{(3)}} r e^{\lambda r} Y_1^0$ and $\chi_2 = -\frac{1}{\sqrt{(3)}} r^2 e^{\lambda r} Y_1^0$. With these basis functions, the polarizability can be calculated and a variational maximum with respect to λ can be found. In Figure 3.1, the exact ground-state polarizability of hydrogen, which is $\alpha = \frac{9}{2}a_0^3$ is obtained at the maximum $\lambda = 1$. There is a region of variational stability between 0.6 and 1.0 where the value of the polarizability is close to the exact value, despite $\lambda \neq 1$. With only two pseudostates needed to obtain the exact value for hydrogen, it is clearly advantageous to use the pseudospectral method instead of the actual spectrum for these types of calculations.

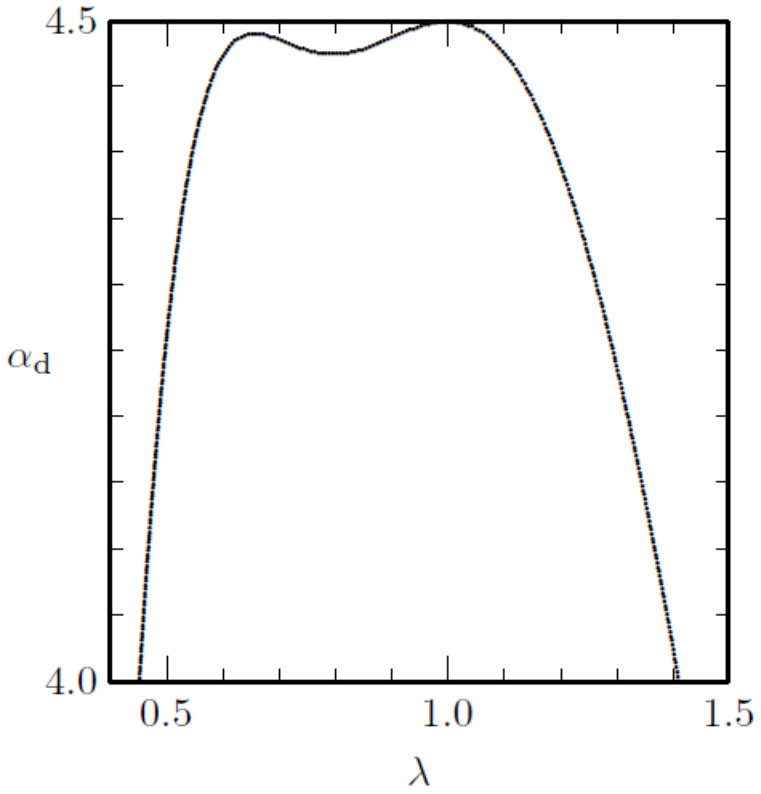

Figure 3.1: The static polarizability of hydrogen as a function of the non-linear parameter lambda. The variational maximum occurs at $\lambda = 1$. [4]

3.4 Relativistic Polarizability

Relativistic corrections to the polarizability are needed to compute a more accurate tune-out wavelength. These corrections contribute to the energy by about an order of α^2 or $\frac{1}{c^2}$ in a.u. thus will contribute significantly to the polarizability. There are multiple ways of applying these corrections; using the Dirac Equation and perturbing the Schrödinger Hamiltonian are two common examples. For these calculations, the second method was used, which involved adding relativistic perturbations to the Schrödinger Hamiltonian. Applying the Dirac Hamiltonian directly onto Schrödinger states will result in erroneous eigenvalues. This is because the Dirac spectrum is not bounded from below. As a result, every bound state is infinitely degenerate for a two

electron atom. For example, if the energy for a given two electron state is close to mc^2, then any combination of the two electron energies that add up to the energy which is close to mc^2 will also be eigenstates, even states that lie above or below the positive or negative continuum. One method to curb this variational collapse is to use configuration interaction (CI) wave functions

$$\psi(\mathbf{r}_1,\mathbf{r}_2) = C_0 u_1^{(s)}(r_1)u_2^{(s)}(r_2) + C_1 u_1^{(P)}(\mathbf{r}_1)u_2^{(P)}(\mathbf{r}_2)\mathcal{Y}^0_{1,1,0}(\hat{\mathbf{r}}_1,\hat{\mathbf{r}}_2) + ... \pm (1 \leftrightarrow 2) \tag{3.23}$$

which exclude negative energy states, but this method is slowly convergent and less accurate [8]. The other method is to perturb the Schrödinger Hamiltonian with relativistic corrections and use Hylleraas functions. This method converges more quickly and is more accurate because the Hylleraas functions not only include all of the terms in the CI wave functions which only contain the even powers of r_{12}, but also the odd powers of r_{12}, which contain all of the powers of $\cos\theta$ due to the Taylor expansion of the cosine law $r_{12} = \sqrt{r_1^2 + r_2^2 - 2r_1 r_2 \cos\theta}$ about $\cos\theta$. Thus, perturbing the Schrödinger Hamiltonian will give a more accurate relativistic correction to the polarizability.
To derive the relativistic dynamic polarizability for a state $|\psi\rangle$, it is useful to start with a slightly modified version of Eq.(3.19) where the relativistic perturbation is added.

$$\alpha_{TOT}(\omega) = e^2(\langle\psi|z\frac{1}{(H_0+H_{rel}) - (E+\langle H_{rel}\rangle) + \hbar\omega}z|\psi\rangle \tag{3.24}$$

$$+\langle\psi|z\frac{1}{(H_0+H_{rel}) - (E+\langle H_{rel}\rangle) - \hbar\omega}z|\psi\rangle) \tag{3.25}$$

The resolvent operator can be geometrically expanded

$$\begin{aligned}\frac{1}{(H_0+H_{rel}) - (E+\langle H_{rel}\rangle) \pm \hbar\omega} =& \frac{1}{H_0 - E_0 \pm \hbar\omega}\times \\ & (\frac{1}{1 + (H_{rel} - \langle H_{rel}\rangle)\frac{1}{H_0 - E_0 \pm \hbar\omega}}) \\ \approx& \frac{1}{H_0 - E_0 \pm \hbar\omega}\times \\ & (1 - (H_{rel} - \langle H_{rel}\rangle)\frac{1}{H_0 - E_0 \pm \hbar\omega})\end{aligned} \tag{3.26}$$

Next is to expand $|\psi\rangle$ to the first order perturbation in H_{rel}.

$$|\psi\rangle = |\psi^0\rangle - \frac{1}{H_0 - E_0} H_{rel} |\psi^0\rangle \tag{3.27}$$

Finally, to obtain the relativistic dynamic polarizability, the expanded resolvent operator and the perturbed wave function are inserted into the expression for $\alpha_{TOT}(\omega)$ (3.24).

$$\begin{aligned}\alpha_{TOT}(\omega) =& e^2(\overbrace{\langle\psi^0|z\frac{1}{H_0 - E_0 + \hbar\omega}z|\psi^0\rangle}^{\text{The positive } \hbar\omega \text{ term in the nonrelativistic } \alpha_{NR}(\omega)} \\ &+2\langle\psi^0|H_{rel}\frac{1}{E_0 - H_0}z\frac{1}{H_0 - E_0 + \hbar\omega}z|\psi^0\rangle \\ &+\langle\psi^0|z\frac{1}{H_0 - E_0 + \hbar\omega}(\langle H_{rel}\rangle - H_{rel})\frac{1}{H_0 - E_0 + \hbar\omega}z|\psi^0\rangle \\ &+[+\hbar\omega \mapsto -\hbar\omega])\end{aligned} \tag{3.28}$$

Thus, the expression for the relativistic dynamic polarizability is $\alpha_{rel}(\omega) = \alpha_{TOT}(\omega) - \alpha_{NR}(\omega)$ where 'NR' means 'nonrelativistic'. Just as in section 3.2, for computing purposes, pseudospectral intermediate states are inserted inbetween the resolvent operator and the appropriate operators to obtain the following expression.

$$\begin{aligned}\alpha_{REL} =& e^2\Big\{ -2\frac{(E_j - E_0)\langle\psi^0|H_{rel}|i\rangle\langle i|z|j\rangle\langle j|z|\psi^0\rangle}{(E_i - E_0)((E_j - E_0)^2 + (\hbar\omega)^2)} \\ &+\frac{\langle\psi^0|z|j\rangle\langle j|(\langle H_{rel}\rangle - H_{rel})|k\rangle\langle k|z|\psi^0\rangle}{((E_j - E_0)^2 - (\hbar\omega)^2)((E_i - E_\psi)^2 - (\hbar\omega)^2)}\times \\ &\big[(E_j - E_0)(E_k - E_0) + (\hbar\omega)^2\big]\Big\}(\text{summation implied})\end{aligned} \tag{3.29}$$

This is the expression that is used to compute the tune-out wavelength, where $\alpha_{TOT} = 0$. The Hamiltonian denoted as H_{rel} represents a sum of relativistic perturbations which include the relativistic kinetic energy, spin-orbit, the Dirac-delta functions and the Breit interaction. These interactions arise from expanding the relativistic energy and will be discussed in the next section.

Chapter 4

Relativistic Hamiltonian

The relativistic corrections to the nonrelativistic Hamiltonian begin with the Darwin Hamiltonian, which was first derived by C.G. Darwin, who was Charles Darwin's grandson. It is a valid description of the interaction between charges up to the order of $\frac{v^2}{c^2}$. By expanding the charge density to second order in retarded time, the Darwin Hamiltonian, which contains a term that is the classical analogue of the Breit interaction, is obtained. The usual treatment of turning a classical Hamiltonian into a quantum one, where the classical variables are replaced with quantum operators, is employed and the result is the Breit interaction itself.

Incorporating the Breit interaction into the Dirac equation provides a relativistic Hamiltonian containing all corrections of order $\frac{v^2}{c^2}$. This Dirac Hamiltonian is then expanded into a Schrödinger Hamiltonian of order $\frac{v^2}{c^2}$ in order to use Hylleraas wave functions. The main advantage of using the Schrödinger Hamiltonian over the Dirac Hamiltonian is the fact that the energies from the Hylleraas wave functions converge much faster than the energies from the relativistic configuration interaction (CI) wave functions which come from solving the Dirac Equation.

The full relativistic Hamiltonian that contains all of the perturbations of order $\frac{v^2}{c^2}$ is comprised of the relativistic kinetic energy, the orbit-orbit interaction, the fine struc-

ture splitting and the relativistic finite mass energy shift.

4.1 Darwin Hamiltonian

The following Hamiltonian describes the interaction between a charge and an external field.

$$H = e\phi - \frac{e}{c}\vec{A}\cdot\vec{v} \tag{4.1}$$

The aim is to obtain a Hamiltonian that describes the interaction between one electron with the field of the other. In order to do this to the order of $\frac{1}{c^2}$, retardation effects must be considered. The scalar and vector potentials are shown below with the charge density as a function of retarded time inserted into the integrals.

$$\phi = \int dV \frac{\rho(t - R/c)}{R} \quad , \quad \vec{A} = \frac{1}{c}\int dV \frac{\rho(t-R/c)\vec{v}}{R} \tag{4.2}$$

The charge density in the ϕ integral is expanded about R/c in order to obtain ϕ to the order of $\frac{1}{c^2}$. The vector potential $\vec{A}$ is not expanded since it already contains a factor of $\frac{1}{c}$, so when it is substituted into the Hamiltonian, the corresponding term will already be of order $\frac{1}{c^2}$. The scalar and vector potentials for an electron are then

$$\phi = \frac{e}{R} + \frac{e}{2c^2}\frac{\partial^2 R}{\partial t^2} \quad , \quad \vec{A} = \frac{e\vec{v}}{cR}. \tag{4.3}$$

Next, a function $f = \frac{e}{2c}\partial_t R$ is constructed in order to simplify the scalar potential by way of the gauge transformation

$$\phi' = \phi - \frac{1}{c}\frac{\partial R}{\partial t} \quad , \quad \vec{A}' = \vec{A} + \nabla f \tag{4.4}$$

The scalar and vector potenials become

$$\phi' = \frac{e}{R} \quad , \quad \vec{A}' = \frac{e\vec{v}}{cR} + \frac{e}{2c}\dot{\hat{n}} \tag{4.5}$$

The vector potential can be further manupulated into something that resembles part of the Breit interaction.

$$\begin{aligned} \vec{A}' &= \frac{e\vec{v}}{cR} + \frac{e}{2c}\frac{\hat{R}}{R} \\ &= \frac{e\vec{v}}{cR} + \frac{e}{2c}(\frac{\dot{\vec{R}}}{R} - \frac{\vec{R}\dot{R}}{R^2}) \\ &= \frac{e[\vec{v} + (\vec{v}\cdot\hat{n})\hat{n}]}{2cR} \end{aligned} \tag{4.6}$$

Finally, the newly gauge transformed potentials are inserted back into 4.1 to obtain the Darwin Hamiltonian for two electrons.

$$H = \frac{e}{R_{12}} - \frac{e^2}{2c^2 R_{12}}[\vec{v_1} \cdot \vec{v_2} + (\vec{v_1} \cdot \hat{n})(\vec{v_2} \cdot \hat{n})] \tag{4.7}$$

[12]

As mentioned before, this Hamiltonian was first derived by Charles Darwin's grandson [13]. The last term can be thought of as the classical analogue to the Breit interaction. Following the usual protocol of turning a classical Hamiltonian into a quantum one, the classical variables are replaced with their corresponding quantum operators. To obtain the Breit interaction, the classical velocities are replaced by the velocity operators $c\vec{\alpha_i}$. The Breit interaction is then

$$B \equiv -\frac{e^2}{2R_{12}}[\vec{\alpha_1} \cdot \vec{\alpha_2} + (\vec{\alpha_1} \cdot \hat{n})(\vec{\alpha_2} \cdot \hat{n})] \tag{4.8}$$

Since the Breit interaction is only valid up to the order of $\frac{v^2}{c^2}$, it would suffice to find a Schrödinger operator U^{eff} which gives the same results up to this order. To do this, the following integral is calculated

$$\langle \psi_C \psi_D | \frac{e^2}{r_{12}} + B | \psi_A \psi_B \rangle = \int\int \Phi_C^*(\vec{r_1}) \Phi_D^*(\vec{r_2}) U^{\text{eff}} \Phi_A(\vec{r_1}) \Phi_B(\vec{r_2}) d^3\vec{r_1} d^3\vec{r_2} + O(\frac{1}{c^4}) \tag{4.9}$$

where $|\psi\rangle = \begin{bmatrix} \varphi \\ \chi \end{bmatrix}$, $\varphi \approx (1 - \frac{p^2}{8m^2c^2})\Phi$ and Φ is a solution to the Schrödinger Hamiltonian. Although the wave functions in practice are not separable, the exact solution can be expressed as a sum of separable functions. The above integral in Eq.(4.9) actually comes from the following integral

$$\langle \Psi_2 | \frac{e^2}{r_{12}} + B | \Psi_1 \rangle \tag{4.10}$$

where $\Psi(\vec{r}_1, \vec{r}_2) = \sum_{A,B} c_{A,B} \psi_A(\vec{r}_1) \psi_B(\vec{r}_2)$. To derive the operator U^{eff}, it suffices to just perform the integral of the one term in (4.9) since only the orders up to $\frac{1}{c^2}$ are of

concern. Putting all the terms together, the approximate Hamiltonian U^{eff} is

$$
\begin{aligned}
U^{\text{eff}} = & \frac{e^2}{r_{12}} - \frac{\pi e^2}{m^2 c^2}\delta^3(\vec{r}_{12}) \\
& \left.\begin{aligned} - \frac{e^2}{2m^2c^2}[\frac{1}{r_{12}}\vec{p}_1 \cdot \vec{p}_2 + \frac{1}{r_{12}^3}\vec{r}_{12} \cdot (\vec{r}_{12} \cdot \vec{p}_2)\vec{p}_2] \end{aligned}\right\} \text{ orbit-orbit } H_{OO} \\
& \left.\begin{aligned} -\frac{e^2}{4m^2c^2r_{12}^3}[\vec{r}_{12} \times \vec{p}_1 \cdot \vec{\sigma}_1 - \vec{r}_{12} \times \vec{p}_2 \cdot \vec{\sigma}_2 \\ +2\vec{r}_{12} \times \vec{p}_1 \cdot \vec{\sigma}_2 - 2\vec{r}_{12} \times \vec{p}_2 \cdot \vec{\sigma}_1] \end{aligned}\right\} \text{ spin-other-orbit } H_{SOO} \\
& \left.\begin{aligned} +\frac{e^2}{4m^2c^2}[\frac{\vec{\sigma}_1 \cdot \vec{\sigma}_2}{r_{12}^3} - 3\frac{(\vec{\sigma}_1 \cdot \vec{r}_{12})(\vec{\sigma}_2 \cdot \vec{r_{12}})}{r_{12}^5} \\ -\tfrac{8\pi}{3}\vec{\sigma}_1 \cdot \vec{\sigma}_2\delta^3(\vec{r}_{12})] \end{aligned}\right\} \text{ spin-spin } H_{SS}
\end{aligned}
\tag{4.11}
$$

The approximated Breit interaction is composed of 3 main parts which are self explanatory. The orbit-orbit interaction describes the coupling between the orbital angular momenta of the two electrons and the spin-other-orbit interaction describes the coupling between the spin of one electron with the orbital angular momentum of the other one. The spin-spin interaction resembles the dipole interaction term in the multipole expansion with the addition of the $\delta^3(\vec{r}_{12})$ term, which is nonzero when the two electrons are in the same position.

Though the Breit interaction accounts for interactions between the two electrons, it does not account for an electron's own spin-orbit coupling. This comes from the Dirac Equation. Like the Breit interaction, the Dirac Hamiltonian can also be expanded into Schrödinger operators of order $\frac{1}{c^2}$ where the spin-orbit coupling becomes apparent.

4.2 The Expanded Dirac Hamiltonian

The Dirac Hamiltonian for a particle in a central field is

$$H = c\vec{\alpha} \cdot \vec{p} + \beta mc^2 + V. \tag{4.12}$$

When H is applied to a 4-component wave function $|\psi\rangle = \begin{bmatrix} \varphi \\ \chi \end{bmatrix}$, a system of two equations is produced

$$(E' - V)\varphi - c\vec{\sigma} \cdot \vec{p}\chi = 0 \tag{4.13}$$

$$(E' + 2mc^2 - V)\chi - c\vec{\sigma} \cdot \vec{p}\varphi = 0 \tag{4.14}$$

[14]

Using these two equations, the small component of the wave function χ can be expressed in terms of the large component φ

$$\chi = \frac{(\vec{\sigma} \cdot \vec{p})}{E' - V + 2mc^2}\varphi \tag{4.15}$$

where $E' \equiv E - mc^2$. To obtain the expanded Dirac Hamiltonian, the denominator

in χ is expanded to order $\frac{1}{c^2}$ and inserted back into the Dirac Equation. The result is the Hamiltonian

$$H\varphi = (\frac{1}{2}p^2 - \frac{\alpha^2}{8}p^4 + \alpha^2\pi\delta^3(\vec{r}) - \frac{\alpha^2}{2}\frac{1}{r}\frac{dV}{dr}\vec{L}\cdot\vec{S})\varphi \tag{4.16}$$

[14]

This expansion brings about three contributions of the order $\frac{1}{c^2}$, which are the p^4, $\delta^3(\vec{r})$ and the spin orbit term H_{SO}. The p^4 term comes from expanding the relativistic kinetic energy $E = \sqrt{(pc)^2 + (mc^2)^2}$. It plays the role of the relativistic change in mass of the electron due to its motion. The $\delta^3(\vec{r})$ term comes from when the electron is in the same position as the nucleus. Finally, the spin-orbit term is the coupling between the electronic orbital and spin angular momenta.

Now, by extending the Dirac Equation to two electrons and including the Breit interaction, a total Hamiltonian containing all corrections of order $\frac{v^2}{c^2}$ is obtained. Again, it is worth mentioning that the unexpanded Dirac Equation could have been used to obtain solutions, but because of the limited accuracy of CI, the Schrödinger Equation with Hylleraas wave functions is used. The power of the latter method over CI is shown in the comparison between our data and data from Zhang et al in the next chapter. Since the Schrödinger operators yield upper bounds to the true energies according to the Hylleraas-Unheim-MacDonald Theorem, the solutions become more precise as $N \to \infty$ [10].

Putting all of the $\frac{1}{c^2}$ order corrections together, the total relativistic Hamiltonian is

$$H_{rel} = \sum_{i=1}^{6} H_i \tag{4.17}$$

where each individual perturbation is shown below [5].

$$H_1 = \frac{\alpha^2}{8}(\vec{p_1}^4 + \vec{p_2}^4)$$

$$H_2 = H_{OO}$$

$$H_3 = H_{SO} + H_{SOO}$$

$$H_4 = \alpha^2\pi\delta^3(\vec{r_1}) + \alpha^2\pi\delta^3(\vec{r_2}) + \alpha^2\pi\delta^3(\vec{r_{12}})$$

$$H_5 = H_{SS}$$

$$H_6 = H_{\text{Stone}}$$

It should be noted that H_6, known as the Stone Term [15], is the finite mass correction to the orbit-orbit and spin-orbit interactions H_2 and H_3. The derivation of this term is similar to the derivation of the mass polarization term in the nonrelativistic three body Hamiltonian and is discussed in the appendix. Now that a working Schrödinger Hamiltonian has been constructed which contains all of the $\frac{1}{c^2}$ ordered effects, the relativistic polarizability can be calculated by substituting this newly expressed H_{rel} into Eq.(3.28).

Chapter 5

The Tune-out Wavelength

The whole purpose of computing the relativistic perturbations is to test QED. In order to do this, all of the lower order perturbations are required because what is observed in nature is the measurement containing all of the approximations. The tune-out wavelength is no exception.

First, the finite and infinite mass nonrelativistic polarizabilities were computed. Each relativistic correction was then added in separately and then the results were compared with values from the literature. This was first done with the ground state of helium in order to be sure that the calculations for polarizability were correct. Once the results were compared with Sapirstein and Pachucki [16], calculations for the $2\ ^3\mathrm{S}$ state proceeded. Calculations for this state underwent the same procedure of computing the perturbations for polarizability separately with the addition of doing the same for the actual tune-out wavelength. These results were compared with the theory work of Zhang et al. and Baldwin's experimental results [7] [2]. Zhang's method of computing the tune-out wavelength involved using an approximate two-electron Dirac Hamiltonian with the Breit interaction in the form expressed in Eq. (4.8). The advantages of the Schrödinger method over this one will be discussed as well as details of the actual measurement of the tune-out wavelength done by Baldwin.

5.1 Measurement

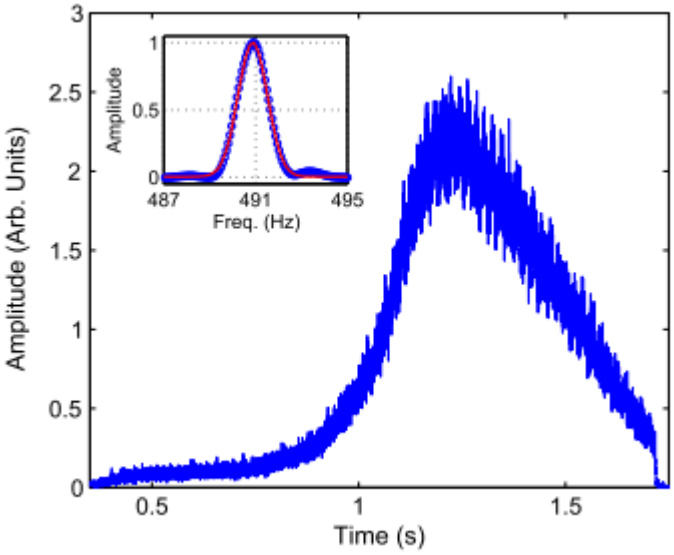

Figure 5.1: The TOF signal of outputted atoms at the laser modulation frequency of 491 Hz. [2]

Several experiments have been done in the recent past that measure the tune-out wavelength. This includes measuring tune-out wavelengths of alkali metals and helium [17] [2]. Since the alkali metals that were used contain many particles, they are not practical candidates for testing QED. Since the crux of this project is to test QED, the measurement of the helium tune-out wavelength is of most interest. In particular, the 413 nm tune-out wavelength is the most sensitive to QED effects because the negative contribution to the polarizability from the virtual 2 ^{3}S to 2 ^{3}P transition dominates and cancels with the positive contributions from the 3 ^{3}P and higher states. Furthermore, other tune-out wavelengths which are close to the 2 ^{3}P triplet states are determined by the 1:3:5 ratio between the corresponding oscillator strengths and are thus, not useful candidates for testing QED since the only major contributions to those tune-out wavelengths are the transitions to the different triplet P states [6]. The 1:3:5 ratio is just the ratio between the oscillator strengths of the 2 ^{3}S to 2 ^{3}P$_0$ transition to that of the 2 ^{3}P$_1$ and 2 ^{3}P$_2$ transitions.

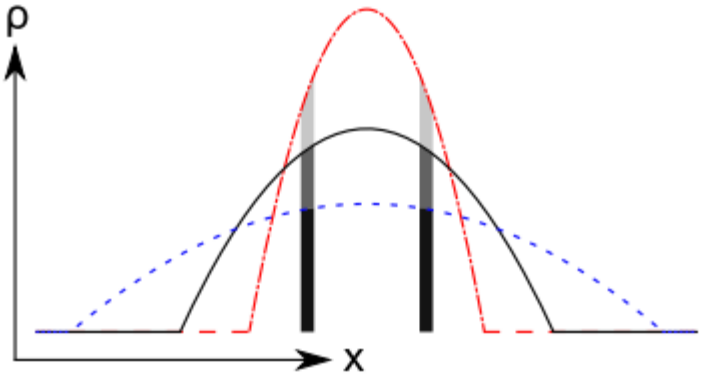

Figure 5.2: Schematic of various one dimensional atomic density beam profiles. The black solid line represents purely magnetically trapped helium. The red dot-dashed line represents a laser potential [sic.] that increases detection rate. The blue dashed line represents a laser potential that decreases detection rate. [2]

The measurement of the 413 nm wavelength itself consists of measuring the effects of a laser on the trapping potential of metastable helium [6]. Basically, a beam helium from a Bose-Einstein condensate is detected on an outcoupling surface and an illuminating laser beam which is meant to perturb the helium beam is tuned until the helium beam profile is the same as the unperturbed beam. This wavelength is then determined to be the tune-out wavelength.

The apparatus consists of a magnetic trap which filters out the atoms in the $m = 0$ substate. Those atoms then fall into a delay line detector (DLD) whereby a time of flight (TOF) signal is measured (Figure 5.1). To account for background noise, the integral of the unperturbed Fourier transformed signal was subtracted from that of the perturbed one. The probing laser is then sweeped in wavelength to find the correct one that yields the unperturbed matter beam profile as shown in Figure 5.2. According to the phase and amplitude data in Figure 5.3, the tune-out wavelength was measured to be $413.0878(9_{\text{stat}})$ nm. With the asymmetry of the peak laser wavelength and the Zeeman splitting in the trap taken into account, the corrected tune-out wavelength was measured to be $413.0938(9_{\text{stat}})(20_{\text{sys}})$ nm [2]. Since the tune-out wavelengths at

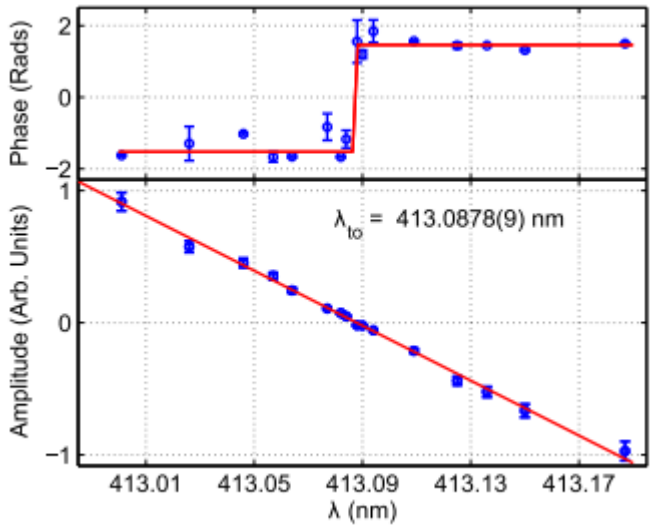

Figure 5.3: Phase and amplitude plotted against laser wavelength. The phase data determines the sign of the amplitude. The amplitude is normalized by the average power. [2]

the different magnetic substates ($m = 0$ and $m = \pm 1$) experimentally differ by only an estimated 2 pm, the difference can be ignored.

5.2 Results

The computation of the tune-out wavelength of ^{4}He is a process that first involves computing the polarizability, and then finding the root of the polarizability closest to the desired transition to obtain the tune-out wavelength. These calculations are split into separate perturbations to show their individual contributions.

In order to verify the calculations, the ground state polarizability, with all of its perturbations, was computed and compared with calculations by Sapirstein, Pachucki and Pukalski [16] [18].

The table below shows the static polarizability, i.e. the polarizability at zero frequency, of ground state ^{4}He and the contributing p^4, the orbit-orbit H_2 term, the Dirac-Delta terms from H_4, the spin dependent terms from H_3 and H_5 and the relativistic finite

mass term. The H_{Stone} term is contained in the relativistic finite mass term, which comprises of the finite mass contributions to the p^4, H_2, the delta function terms, the spin-dependent terms and the whole H_{Stone} term. Precisely speaking, the p^4 term is the contribution to the polarizability from H_1, the $\delta^3(r_1)$ term is the contribution from $\pi\delta^3(r_1) + \pi\delta^3(r_2)$ and the $\delta^3(r_{12})$ term is the contribution from $\pi\delta^3(r_{12})$. Since the wave functions that are used are antisymmetric, $\langle\delta^3(r_2)\rangle = \langle\delta^3(r_2)\rangle$ which is why both the $\delta^3(r_1)$ and $\delta^3(r_2)$ terms are described $\delta^3(r_1)$ in the table. The total is then the sum of all of the perturbations listed the tables except for the H_{Stone} term, since it is already contained in the relativistic finite mass term. For the singlet ground state, the spin dependent contributions are zero so they are not listed. The number Ω controls the size of the basis set that was used as intermediate states. The convergence ratios, which are the ratios between the sequential differences, indicate that the limiting factors to the convergence of the total are the relativistic polarizabilities. The ratio is defined by $\frac{\alpha(\Omega(M+1))-\alpha(\Omega(M))}{\alpha(\Omega(M+2))-\alpha(\Omega(M+1))}$. The convergence uncertainty is calculated by taking the median of the convergence ratios and using that ratio to compute an infinite series assuming that all subsequent differences have the same ratio. This infinite series is equal to the difference between the extrapolated value and the value corresponding to the median ratio. The uncertainty is then twice this value. All of the polarizabilities are in units of a_0^3.

5.2.1 Ground State Polarizability

These are the results for the different contributions to the ground state static polarizability of ^{4}He, namely the nonrelativistic, p^4, orbit-orbit, the delta function terms from H_4 and the finite mass contributions. Even though the tune-out wavelength corresponds to the polarizability of the 2 ^{3}S state, the ground state polarizability was calculated because the various contributions to the ground state polarizability of ^{4}He are already known in the literature [18] [16]. This allows for a comparison with literature to show that our method of calculation is working properly.

Table 5.1: Ground State Polarizability: Nonrelativistic and p^4 Terms

$\Omega(N)$	NR (a_0^3)	Ratio	p^4 (10^{-6} a_0^3)	Ratio
4	1.38319212217577		-988.12723	
5	1.38319216773268		-988.09352	
6	1.38319217273427	9.11	-987.92470	0.20
7	1.38319217389379	4.31	-987.91715	22.35
8	1.38319217436197	2.48	-987.88049	0.21
9	1.38319217441845	8.29	-987.89107	-3.47
10	1.38319217444475	2.15	-987.87775	-0.79
11	1.38319217445109	4.15	-987.87672	12.98
12	1.38319217445374	2.39	-987.87559	0.90
13	1.38319217445437	4.21	-987.87634	-1.50

Table 5.2: Ground State Polarizability: Orbit-Orbit and $\delta^3(r_1)$ Terms

$\Omega(N)$	H_2 (10^{-6} a_0^3)	Ratio	$\delta^3(r_1)$ (10^{-6} a_0^3)	Ratio
4	–23.234218359		864.80946	
5	–23.234015044		864.78833	
6	–23.234066054	–3.99	864.70454	0.25
7	–23.234049037	–3.00	864.70023	19.45
8	–23.234062109	–1.30	864.68224	0.24
9	–23.234054740	–1.77	864.68728	–3.57
10	–23.234058328	–2.05	864.68068	–0.76
11	–23.234057559	–4.66	864.68014	12.20
12	–23.234057465	8.17	864.67957	0.94
13	–23.234057839	–0.25	864.67997	–1.44

Table 5.3: Ground State Polarizability: $\delta^3(r_{12})$ and Nonrelativistic Finite Mass Terms

$\Omega(N)$	$\delta^3(r_{12})$ (10^{-6} a_0^3)	Ratio	NR Finite Mass (10^{-6} a_0^3)	Ratio
4	66.078388		617.812093590020	
5	66.069868		617.811950980096	
6	66.071347	–5.76	617.811947229985	38.03
7	66.070284	–1.39	617.811943320001	0.96
8	66.071049	–1.39	617.811943400159	–48.78
9	66.070546	–1.52	617.811946119984	0.03
10	66.070694	–3.40	617.811945790026	–8.24
11	66.070642	–2.81	617.811946375314	–0.56
12	66.070631	4.69	617.811946384850	61.38
13	66.070674	–0.26	617.811946419966	0.27

Table 5.4: Ground State Polarizability: Stone Term and Total Polarizability

$\Omega(N)$	H_{Stone} (10^{-6} a_0^3)	Ratio	Total (a_0^3)	Ratio
4	–.24932414		1.383729367558	
5	–.24933533		1.383729415756	
6	–.24933407	–8.91	1.383729508298	0.520824734
7	–.24933248	0.79	1.383729511778	26.58929882
8	–.24933236	13.33	1.383729531617	0.175433242
9	–.24933210	0.47	1.383729525587	–3.289883466
10	–.24933219	–2.99	1.383729532519	–0.869825623
11	–.24933212	–1.20	1.383729533076	12.44988963
12	–.24933212	63.50	1.383729533282	2.707632046
13	–.24933211	0.19	1.383729533126	–1.320207935

Table 5.5: Ground State Polarizability: Relativistic Finite Mass Terms

$\Omega(N)$	Relativistic Finite Mass ($10^{-8}\ a_0^3$)	Ratio
4	–9.30764	
5	–9.45678	
6	–9.34808	–1.37
7	–9.33548	8.63
8	–9.34029	–2.62
9	–9.34584	0.87
10	–9.34232	–1.58
11	–9.3307	0.30
12	–9.36535	–0.34
13	–9.34972	–2.22

Table 5.6: Ground State Polarizability: Summary

Contribution	Polarizability (a_0^3)	Absolute Percentage to Total
NR	1.38319217445437(83)	99.961166%
p^4 (10^{-6})	–987.87634(45)	0.071392%
$\delta^3(r_1)$ (10^{-6})	864.67997(23)	0.062489%
NR Finite Mass (10^{-6})	617.811 94641(4)	0.044648%
$\delta^3(r_{12})$ (10^{-6})	66.070 67(4)	0.004775%
H_2 (10^{-6})	–23.234 05784(38)	0.001679%
Relativistic Finite Mass (10^{-8})	–9.35(1)	0.000007%
Total	1.38372953313(9)	
H_{Stone} (10^{-6})	–0.24933211(2)	–0.000018%

The contributions from the nonrelativistic to the relativistic finite mass in Table

5.6 are listed from largest absolute value to the least. The most dominant relativistic contribution comes from the p^4 term which accounts for about 0.0714 % of the total polarizability and the smallest contribution comes from relativistic finite mass corrections, which are of the order $\alpha^2 \frac{\mu}{M}$.

The contribution that limits the convergence the most is the p^4 term as shown in 5.6 whose convergence uncertainty of $9 \times 10^{-9}\ a_0^3$ is the largest one out of all of the other contributions. The other contributions that are limitting the convergence accuracy are the other relativistic contributions with the exception of the relativistic finite mass term. The average uncertainty of the relativistic contributions except for the Stone term is $35 \times 10^{-10}\ a_0^3$, which is approximately 300 times larger than the uncertainty of the nonrelativistic contribution. Collectively, the uncertainties of the relativistic contributions bring the uncertainty up from 12×10^{-12} to 9×10^{-11}, making them the most significant factors in limiting the convergence accuracy. The same applies for the $2\ ^3$ S case.

5.2.2 $2\ ^3$S Polarizability

These are the different contributions to the polarizability of the $2\ ^3$S state of helium. The spin-orbit and spin-other-orbit contributions from H_3 are zero and so they are not listed. Unlike the case for the singlet ground state, the polarizability for the $2\ ^3S_1$ state has components for $m = 0$ and $m = \pm 1$ because of the angular momentum selection rules.

Table 5.7: 2 ^{3}S Polarizability: Nonrelativistic and p^4 terms

$\Omega(N)$	NR (a_0^3)	Ratio	p^4 (a_0^3)	Ratio
4	315.6309700019458910519		–0.2697741791055096319	
5	315.6314392635272574374		–0.2697786448622702241	
6	315.6314682938799325927	16.16	–0.2697814471322769431	1.59
7	315.6314717952392098448	8.29	–0.2697833828452446287	1.45
8	315.6314722224723372132	8.20	–0.2697836574270027043	7.05
9	315.6314723432909492929	3.54	–0.2697809023811375977	–0.10
10	315.6314723654509451395	5.45	–0.2697806412975781859	–10.55
11	315.6314723736341903654	2.71	–0.2697818299910386912	–0.22
12	315.6314723757233973916	3.92	–0.2697817546564160514	15.78
13	315.6314723763563185573	3.30	–0.2697815442290065093	0.36
14	315.6314723765413712470	3.42	–0.2697816022466314044	–3.63

Table 5.8: 2 ^{3}S Polarizability: Orbit-Orbit and $\delta^3(r_1)$ Terms

$\Omega(N)$	H_2 (a_0^3)	Ratio	$\delta^3(r_1)$ (a_0^3)	Ratio
4	–0.0111420067907148869		0.1821921447448293390	
5	–0.0111420448415984569		0.1821928967304806717	
6	–0.0111420789862821105	1.11	0.1821943945643147368	0.50
7	–0.0111420811440260406	15.82	0.1821953383942443313	1.59
8	–0.0111420820354247762	2.42	0.1821954784628352565	6.74
9	–0.0111420821523863042	7.62	0.1821941008979720464	–0.10
10	–0.0111420821533393841	122.73	0.1821939710417952776	10.61
11	–0.0111420821453396128	–0.12	0.1821945651351438234	–0.22
12	–0.0111420821399657323	1.49	0.1821945275041228298	–15.79
13	–0.0111420821411552684	–4.52	0.1821944222865652298	0.36
14	–0.0111420821403096014	–1.41	0.1821944512767977097	–3.63

Table 5.9: 2 ^{3}S Polarizability: Nonrelativistic Finite Mass and Stone terms

$\Omega(N)$	NR Finite Mass (a_0^3)	Ratio	H_{Stone} (a_0^3)	Ratio
4	0.18888592456301		–0.0000756586837165675	
5	0.18887735097297		–0.0000756595328050752	
6	0.18887756998100	–39.15	–0.0000756597201414395	4.53
7	0.18887756240702	–28.92	–0.0000756596356824319	–2.22
8	0.18887757023299	–0.97	–0.0000756596080993842	3.06
9	0.18887757009998	–58.84	–0.0000756595657978618	0.65
10	0.18887757034702	–0.54	–0.0000756595505548210	2.78
11	0.18887757033701	–24.69	–0.0000756595743309846	–0.64
12	0.18887757035304	–0.62	–0.0000756595733113076	–23.32
13	0.18887757035799	3.24	–0.0000756595707175300	0.39
14	0.18887757034099	–0.29	–0.0000756595715710384	–3.04

Table 5.10: 2 ^{3}S Polarizability for $m = 0$ Substate: Spin-spin and Relativistic Finite Mass Terms

$\Omega(N)$	H_{SS} (a_0^3)	Ratio	Relativistic Finite Mass (a_0^3)	Ratio
4	–0.0055244407509578922		–0.0000935628957326236	
5	–0.0055241975172654250		–0.0000945001890032644	
6	–0.0055242201262332933	–10.76	–0.0000934162854854571	–0.86
7	–0.0055242166962180999	–6.59	–0.0000936190714712739	–5.35
8	–0.0055242168514690298	–22.09	–0.0000921134011250780 0	–0.13
9	–0.0055242165868716178	–0.59	–0.0000933579253310415	–1.21
10	–0.0055242167489752545	–1.63	–0.0000940912992250060	1.70
11	–0.0055242167883370083	4.12	–0.0000934367090416974	–1.12
12	–0.0055242168491920879	0.65	–0.0000933988059011008	17.27
13	–0.0055242167902125542	–1.03	–0.0000935163153185023	–0.32
14	–0.0055242167889241537	45.78	–0.0000934965791349520	–5.95

Table 5.11: 2 ^{3}S Polarizability for $m = 0$ Substate: Total Polarizability

$\Omega(N)$	Total (a_0^3)	Ratio
4	315.715513839191	
5	315.715970081283	
6	315.715999053414	15.75
7	315.716001353828	12.59
8	315.716003159012	1.27
9	315.716003412774	7.11
10	315.716002832832	–0.44
11	315.716002900991	–8.51
12	315.716002978648	0.88
13	315.716002967041	–6.69
14	315.716002957921	1.27

Table 5.12: $2\,^3$S Polarizability for $m = \pm 1$ Substates: Spin-spin and Relativistic Finite Mass Terms

$\Omega(N)$	H_{SS} (a_0^3)	Ratio	Relativistic Finite Mass (a_0^3)	Ratio
4	0.0027622203754789461		–0.0000864335655261432	
5	0.0027620987586327125		–0.0000873609664674251	
6	0.0027621100631166467	–10.76	–0.0000862771905863081	–0.86
7	0.0027621083481090500	–6.59	–0.0000864796183027740	–5.35
8	0.0027621084257345149	–22.09	–0.0000849745559806481	–0.13
9	0.0027621082934358089	–0.59	–0.0000862184597615707	–1.21
10	0.0027621083744876272	–1.63	–0.0000869520263627561	1.70
11	0.0027621083941685042	4.12	–0.0000862973952627079	–1.12
12	0.0027621084245960440	0.65	–0.0000862596466976806	17.34
13	0.0027621083951062771	–1.03	–0.0000863770907166329	–0.32
14	0.0027621083944620769	45.78	–0.0000863573599562419	–5.95

Table 5.13: 2 ^{3}S Polarizability for $m = \pm 1$ Substates: Total Polarizability

$\Omega(N)$	Total (a_0^3)	Ratio
4	315.723807629648	
5	315.724263516782	
6	315.724292522699	15.72
7	315.724294818326	12.64
8	315.724296623134	1.27
9	315.724296877120	7.11
10	315.724296297229	–0.44
11	315.724296365487	–8.50
12	315.724296443081	0.88
13	315.724296431451	–6.67
14	315.724296422323	1.27

Table 5.14: 2 ^{3}S Polarizability: Summary

Contribution	Polarizability (a_0^3)	Absolute Percentage to Total
NR	315.6314723765(5)	99.973226%
p^4	–0.2697816(3)	0.085451%
NR Finite Mass	0.1888775703(3)	0.059825%
$\delta^3(r_1)$	0.1821944(2)	0.057708%
H_2	–0.011142082140(3)	0.003529%
H_{SS} $(m = 0)$	–0.005524216788(3)	0.001750%
H_{SS} $(m = \pm 1)$	0.002762108394(2)	0.000875%
Relativistic Finite Mass $(m = 0)$	–0.0000934(2)	0.000030%
Relativistic Finite Mass $(m = \pm 1)$	–0.0000863(2)	0.000027%
Total $(m = 0)$	315.71600295(2)	
Total $(m = \pm 1)$	315.72429642(2)	
H_{Stone}	–0.000075659571(1)	0.000024%

The contributions in Table 5.14 are listed from greatest absolute percentage to least just as in Table 5.6. Only the percentages to the total $m = 0$ state for the spin independent terms are shown, since the largest difference between those percentages and the percentages to the total $m = \pm 1$ state is 0.000004%. However, the percentages for the spin dependent terms are the percentages with respect to the total of the respective magnetic substate. The percentages of each contribution are of the same order of magnitude as the percentages of the ground state case in Table 5.6. Furthermore, the contributions for the 2 ^{3}S state rank from greatest to least in a similar order to the ground state. The only difference is that in this case, the nonrelativistic finite mass is larger than the $\delta^3(r_1)$ term.

Similar to Table 5.6, Table 5.14 shows that the perturbation that limits the convergence the most is the p^4 term. Other major contributions to the limiting convergence are the other relativistic spin independent terms such as the orbit-orbit and the delta

function terms.

5.2.3 The $2\ ^3S$ - $3\ ^3P$ Transition Tune-out Wavelength

As mentioned before, tune-out wavelengths are calculated by finding roots of Eq.(3.24) i.e. the dynamic polarizability. The tune-out wavelength that is of interest is the one corresponding to the $2\ ^3S$ - $3\ ^3P$ transition because it is the closest tune-out wavelength to the static polarizability, making it the most accessible experimentally because it is the lowest energy tune-out wavelength for the $2\ ^3S$ state. This tune-out wavelength is also a good candidate for testing QED because of the off diagonal matrix elements used in its calculation.

Other tune-out wavelengths, such as the tune-out wavelengths that lie between the different ^3P_J states are not strong enough candidates for testing QED because their tune-out wavelengths are determined predominantly by the 1:3:5 ratio [2], which is the ratio between the oscillator strengths of the $J = 0$, 1 and 2 multiplet states. Figure 5.4 shows the nonrelativistic polarizability as a function of the frequency of the interacting EM wave.

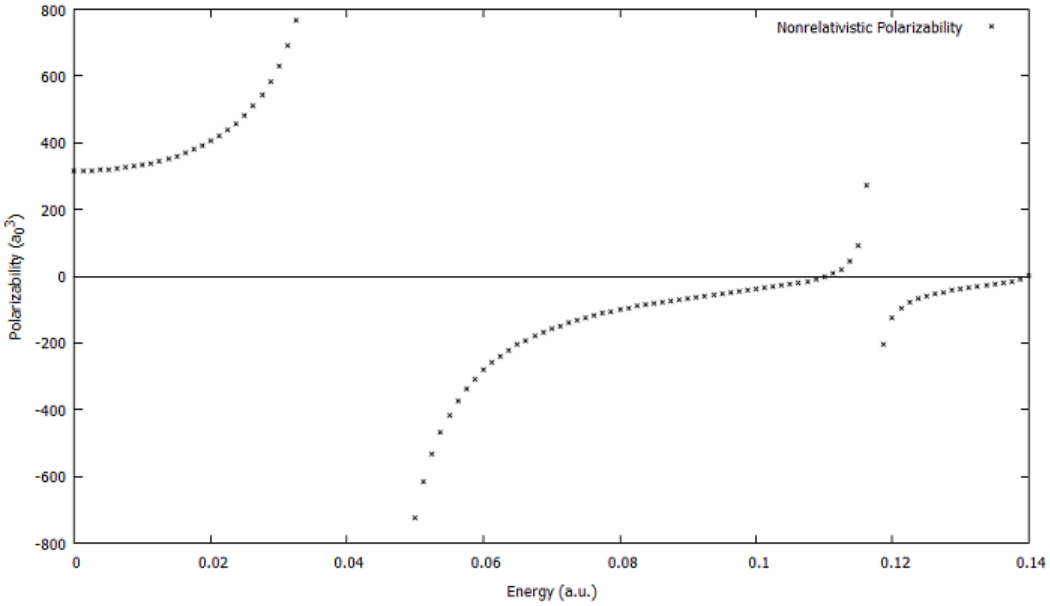

Figure 5.4: Nonrelativistic Dynamic Polarizability of the 2 ^{3}S state as a function of electric field oscillation frequency. The 2 ^{3}S - 3 ^{3}P transition tune-out frequency, in atomic units, is the first zero on the blue side of the static polarizability.

Tables 5.15 - 5.19 correspond to the contributions from the different perturbations to the actual tune-out wavelength. The spin independent term includes the kinetic energy term p^4, the orbit-orbit term H_2 and the delta function terms. Though the Stone term is independent of spin, it is not included in the "Spin Independent" term in Table 5.15 because it has its own heading in Table 5.16. The spin dependent term is just the spin-spin interaction H_{SS}, since the spin-orbit interactions for the 2 ^{3}S state are zero. The roots of the dynamic polarizability were calculated for each perturbation by using Newton's method every time a perturbation was added.

Table 5.15: 2 ^{3}S - 3 ^{3}P Tune-out Wavelength: Nonrelativistic and Spin Independent Terms

$\Omega(N)$	NR (nm)	Ratio	Spin Independent (nm)	Ratio
4	413.039841158627217		–0.0563393905960083	
5	413.038621572579689		–0.0537620561270273	
6	413.038391102846652	5.29	–0.0543741622490188	–4.21
7	413.038344781791459	4.98	–0.0552959422009849	0.66
8	413.038308592527443	1.28	–0.0552623273169957	–27.42
9	413.038305405431768	11.35	–0.0553469393279897	–0.40
10	413.038304554346877	3.74	–0.0553633060729908	5.17
11	413.038304450249554	8.18	–0.0553663883409854	5.31
12	413.038304396407023	1.93	–0.0552695346809742	–0.03
13	413.038304389131702	7.40	–0.0553168531639585	–2.05
14	413.038304386839547	3.17	–0.0552888933340228	–1.69

Table 5.16: 2 ^{3}S - 3 ^{3}P Tune-out Wavelength: Stone and Nonrelativistic Finite Mass terms

$\Omega(N)$	H_{Stone} (10^{-5} nm)	Ratio	NR Finite Mass (nm)	Ratio
4	–4.45548		0.100861132	
5	–4.43728		0.100891719	
6	–4.44167	–4.15	0.100917632	1.18
7	–4.44532	1.20	0.100880904	–0.71
8	–4.44517	–24.01	0.100913888	–1.11
9	–4.44556	–0.39	0.100916219	14.14
10	–4.44566	4.07	0.100916971	3.10
11	–4.44557	–1.01	0.100917022	14.74
12	–4.44521	0.27	0.100917066	1.15
13	–4.44539	–1.94	0.100917072	8.68
14	–4.44531	–2.14	0.100917073	3.18

Table 5.17: 2 ^{3}S - 3 ^{3}P Tune-out Wavelength for $m = 0$ Substate: Spin Dependent and Relativistic Finite Mass Terms

$\Omega(N)$	Spin Dependent (nm)	Ratio	Relativistic Finite Mass (nm)	Ratio
4	–0.003907651		–0.00028599268006246300	
5	–0.00390727		–0.00010957205000750000	
6	–0.003907339	–5.49	–0.00005342177399825230	3.14
7	–0.003907426	0.80	–0.00001657785799125120	1.52
8	–0.003907424	–30.51	–0.00013563902001578800	–0.31
9	–0.003907433	–0.29	–0.00006690985100021860	–1.73
10	–0.003907436	3.80	–0.00005621146897283320	6.42
11	–0.003907437	3.80	0.00000539114091679949	0.17
12	–0.003907424	–0.05	–0.00009588122298964660	–0.61
13	–0.00390743	–1.96	–0.00002327142306057790	–1.39
14	–0.003907426	–1.60	–0.00007028439694067860	–1.54

Table 5.18: 2 ^{3}S - 3 ^{3}P Tune-out Wavelength for $m = 0$ Substate: Total Tune-out Wavelength

$\Omega(N)$	Total (nm)	Ratio
4	413.080169213119028	
5	413.081734368224646	
6	413.080973788888211	–2.06
7	413.080005717958754	0.79
8	413.079917063472789	10.92
9	413.079900318642273	5.29
10	413.079894549905820	2.90
11	413.079953018110609	–0.10
12	413.079948598697846	–13.23
13	413.079973883882201	–0.17
14	413.079954832864554	–1.33

Table 5.19: 2 ^{3}S - 3 ^{3}P Tune-out Wavelength for $m = \pm 1$ Substates: Spin Dependent and Relativistic Finite Mass Terms

$\Omega(N)$	Spin Dependent	Ratio	Relativistic Finite Mass	Ratio
4	0.00195384148901212		–0.0002803957240189450	3.14
5	0.00195365067799003		–0.0001039880469306810	1.52
6	0.00195368543700170	–5.49	–0.0000478444389955257	
7	0.00195372902697954	0.80	–0.0000110052200170685	
8	0.00195372759799284	–30.50	–0.0001300472670209270	–0.31
9	0.00195373248595843	–0.29	–0.0000613290039268577	–1.73
10	0.00195373377300712	3.80	–0.0000506329910194836	6.42
11	0.00195373411202127	3.80	0.0000109572899873456	0.17
12	0.00195372767097979	–0.05	–0.0000902947780332397	–0.61
13	0.00195373096198637	–1.96	–0.0000177004630472766	–1.39
14	0.0019537289070399300	–1.600	–0.000064702996041887	–1.5470

Table 5.20: 2 ^{3}S - 3 ^{3}P Tune-out Wavelength for $m = \pm 1$ Substates: Total Tune-out Wavelength

$\Omega(N)$	Total (nm)	Ratio
4	413.086036302952497	
5	413.087600872628121	
6	413.086840390913203	–2.06
7	413.085872446078808	0.79
8	413.085783806422229	10.92
9	413.085767065351583	5.29
10	413.085761298107101	2.90
11	413.085819755000376	–0.10
12	413.085815336558287	–13.23
13	413.085840616131512	–0.17
14	413.085821569389082	–1.33

The preliminary results for the total relativistic tune-out wavelengths are 413.07997(2) nm and 413.08582(2) nm for the $m = 0$ and $m = \pm 1$ substates respectively. These results were obtained by using the Hylleraas wave functions in Eq.(2.10) as intermediate pseudostates. The nonlinear parameters for these pseudostate functions are optimized with respect to the energy of the 2 ^{3}S state.

The reason why the results in this section are preliminary is because the accuracy can be improved drastically. For instance, the relativistic finite mass contribution, which is $-0.0000647(470)$ nm, has an uncertainty greater than the contribution itself. The convergence accuracy is improved by optimizing the tune-out wavelength with respect to one of the nonlinear parameters. Doing this decreases the convergence uncertainty by over two orders of magnitude, yielding the final results of 413.0799585(4) nm and 413.0858252(4) nm for the different substates. The next section covers the final optimized results in more detail.

5.2.4 Optimized Tune-out Wavelength

The optimization of the tune-out wavelength involves optimizing the intermediate states that are used in its calculation. The Hylleraas wave functions for the intermediate states are

$$\Psi(r_1, r_2, r_{12}) = \sum_{p=1}^{q} \sum_{ijk}^{i+j+k\leq\Omega_q} c_{ijk}^{p} r_1^i r_2^j r_{12}^k \mathcal{Y}_{l_1,l_2,L}^{M}(\hat{r}_1, \hat{r}_2) e^{-\alpha_p r_1 - \beta_p r_2} + (r_1 \leftrightarrow r_2) \quad (5.1)$$

[19]

where the total wave function is split into sectors corresponding to their nonlinear parameters. The functions used to calculate the polarizabilities and tune-out wavelengths had two sectors where q spans the interval $[1, 2]$. The sector 1 nonlinear parameters α_1 and β_1 describe the asymptotic behaviour of the first and second electrons respectively and the sector 2 nonlinear parameters describe the short range behaviour [19]. The parameter that is used to optimize the tune-out wavelength is the long range second electron parameter β_1 for the intermediate S states. This parameter was chosen because it is the nonlinear parameter limiting the convergence of the tune-out wavelength the most. The value of β_1 that optimizes the tune-out wavelength was found by plotting the tune-out wavelength as a function of β_1 as shown in Figure 5.5.

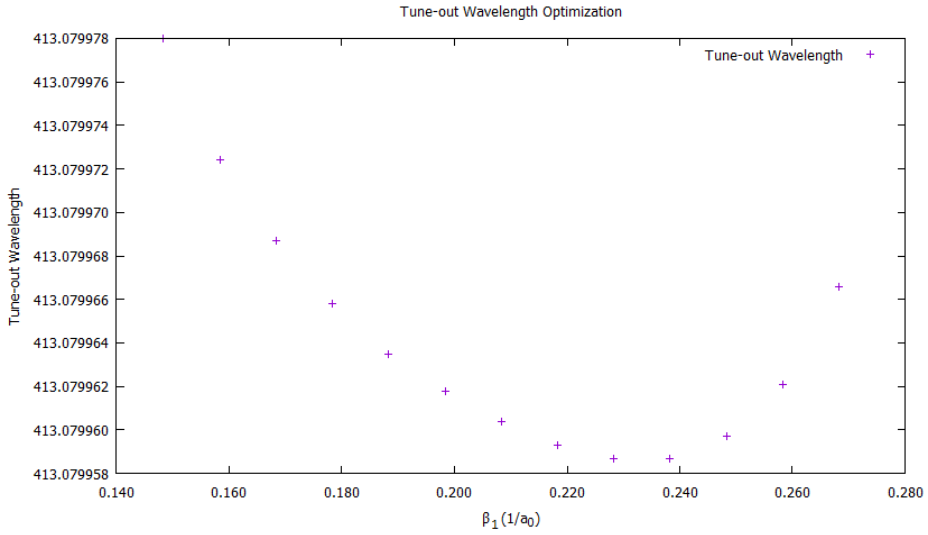

Figure 5.5: Dynamic Polarizability of the 2 ^{3}S state as Tune-out wavelength varied over the nonlinear parameter β_1.

The value for the local minimum, 0.238403 a_0^{-1}, was found by plotting 13 data points and choosing the one which yielded the lowest tune-out wavelength. Finding the tune-out wavelength this way is accurate enough for the purpose of finding the tune-out wavelength since the nonlinear parameter did not need to be accurate beyond six figures. For instance, the calculated energy of the 2 ^{3}S state where $\beta_1 = 0.44336$ is -2.1752291659 a.u. whereas the energy using $\beta_1 = 0.50336$ is -2.1752291657 a.u. The difference in 0.6 a_0^{-1} yielded a difference in energy of only 2×10^{-10} a.u. which is much larger than the relativistic energy of that state, which is about 8.7×10^{-6} a.u. Due to issues with the diagonalization routine producing negative norms, results beyond $\Omega(N) = 11$ could not be obtained.

Table 5.21: Optimized 2 ^{3}S Tune-out Wavelength: Nonrelativistic and p^4 Terms Independent Terms

$\Omega(N)$	NR (nm)	Ratio	p^4 (nm)	Ratio
5	413.038272220752935		–0.15636242335802	
6	413.038301330261326		–0.15635169837202	
7	413.038304063344664	10.65	–0.15635959126001	1.36
8	413.038304368327504	8.96	–0.15635922031498	21.28
9	413.038304414726394	6.57	–0.15635716428500	0.18
10	413.038304395780686	2.45	–0.15635806816499	2.27
11	413.038304399611443	4.95	–0.15635838278701	2.87

Table 5.22: Optimized 2 ^{3}S Tune-out Wavelength: Orbit-Orbit and $\delta^3(r_1)$ Terms

$\Omega(N)$	H_2 (nm)	Ratio	$\delta^3(r_1)$ (nm)	Ratio
5	–0.00886310247699		0.109918641581032	
6	–0.00886313672697		0.109913371336972	
7	–0.00886314262198	5.81	0.109917329174948	1.33
8	–0.00886314296997	16.94	0.109917144988003	21.49
9	–0.00886314295099	18.33	0.109916115602005	0.18
10	–0.00886314314403	0.10	0.109916569962991	2.27
11	–0.00886314307996	3.01	0.109916727217978	2.89

Table 5.23: Optimized 2 ^{3}S Tune-out Wavelength: Nonrelativistic Finite Mass and Stone Terms

$\Omega(N)$	NR Finite Mass (nm)	Ratio	$H_{\rm Stone}$ (nm)	Ratio
5	0.0442875064049986		–0.0000444517220330454	
6	0.0442862808770315		–0.0000444508159489487	
7	0.0442862802769923	2042.41	–0.0000444511009618509	3.18
8	0.0442862639710029	0.04	–0.0000444510890247329	23.88
9	0.0442862373259914	0.61	–0.0000444510479837845	0.29
10	0.0442862130759636	1.10	–0.0000444510740180704	1.58
11	0.0442862147780261	14.25	–0.0000444510679926680	4.32

Table 5.24: Optimized 2 ^{3}S Tune-out Wavelength for $m = 0$ Substate: Spin-Spin and Relativistic Finite Mass Terms

$\Omega(N)$	$H_{\rm SS}$ (nm)	Ratio	Relativistic Finite Mass (nm)	Ratio
5	–0.00390741142797424000		–0.00001717675007739670	
6	–0.00390743217303680000		–0.00000616274195408550	
7	–0.00390743074001421000	14.48	–0.00000530609901261414	12.86
8	–0.00390743104497915000	4.70	–0.00000640731803969175	0.78
9	–0.00390743083102052000	1.43	–0.00000621130197941966	5.62
10	–0.00390743099495694000	1.31	–0.00000631104904869062	1.97
11	–0.00390743100797408000	12.59	–0.00000626897394795378	2.37

Table 5.25: Optimized 2 ^{3}S Tune-out Wavelength for $m = 0$ Substate: Total Tune-out Wavelength

$\Omega(N)$	Total (nm)	Ratio
5	413.079914653151703	
6	413.079958956345020	
7	413.079958606127485	126.50
8	413.079957979629612	0.56
9	413.079959222327930	0.50
10	413.079958629476396	2.10
11	413.079958519778064	5.40

Table 5.26: Optimized 2 ^{3}S Tune-out Wavelength for $m = \pm 1$ Substates: Spin-Spin and Relativistic Finite Mass Terms

$\Omega(N)$	H_{SS} (nm)	Ratio	Relativistic Finite Mass (nm)	Ratio
5	0.00195372150602680000		–0.00005605258706964380	
6	0.00195373187995074000		–0.00004503999690541600	
7	0.00195373116400788000	14.49	–0.00004418399595351730	12.87
8	0.00195373131498400000	4.74	–0.00004528498902800490	0.78
9	0.00195373120897102000	1.42	–0.00004508893891852490	5.62
10	0.00195373129105292000	1.29	–0.00004518872003700380	1.96
11	0.00195373129798782000	11.84	–0.00004514665289434560	2.37

Table 5.27: Optimized 2 ^{3}S Tune-out Wavelength for $m = \pm 1$ Substates: Total Tune-out Wavelength

$\Omega(N)$	Total (nm)	Ratio
5	413.085781361970764	
6	413.085825693959964	
7	413.085825341235329	125.68
8	413.085824715407114	0.56
9	413.085825957778186	0.50
10	413.085825365165616	2.10
11	413.085825255473486	5.40

Table 5.28: 2 ^{3}S Tune-out Wavelengths: Summary

Contribution	Tune-out Wavelength (nm)	Absolute Percentage to Total
NR	413.038304399(9)	99.989916%
p^4	–0.156358(1)	0.037852%
$\delta^3(r_1)$	0.1099167(6)	0.026609%
NR Finite Mass	0.1009170926(3)	0.024430%
H_2	–0.00886314307(15)	0.002146%
H_{SS} $(m = 0)$	–0.00390743100(3)	0.000946%
H_{SS} $(m = 1)$	0.00195373129(2)	0.000473%
Relativistic Finite Mass $(m = 0)$	–0.0000063(2)	0.000002%
Relativistic Finite Mass $(m = 1)$	–0.0000451(2)	0.000011%
Total $(m = 0)$	413.0799585(4)	
Total $(m = 1)$	413.0858252(4)	
H_{Stone}	–0.000044451067(8)	0.000011%

Table 5.28 shows the optimized final results for the 2 ^{3}S - 2 ^{3}P transition tune-out wavelength. The proportions of each perturbation to the total are within the same order of magnitude as the proportions for the 2 ^{3}S static polarizability. The order of the percentages from greatest to least is almost the same as those for the static polarizability case. The difference is that in the tune-out wavelength case, the nonrelativistic finite mass contribution is greater than the delta-function contribution instead of the other way around for the polarizability case.

As for convergence uncertainty, the minimized tune-out wavelengths yielded much better convergence with uncertainties in the tune-out wavelength of about 12×10^{-8} nm as compared with the uncertainty without optimization, which was 2×10^{-5} nm. The final calculated values of the total relativistic tune-out wavelengths for the $m = 0$ and $m = \pm 1$ substates are 413.079 958 5(4) nm and 413.085 825 2(4) nm respectively.

5.3 Comparison With Other Work

In order to verify the method of calculating the polarizability, the polarizability was calculated for the ground state of helium-4 and the results were compared with the results of Puchalski [18] [16]. The nonrelativistic polarizability containing nonrelativistic mass polarization, the contribution from terms of the order α^2 and the contribution from the $\frac{\mu}{M}\alpha^2$ terms were compared with Puchalski's work. As shown in Table 5.29, our calculations agree to 1 part in 10^{12} for the nonrelativistic polarizability and 1 part in 10^{10} for the α^2 and $\frac{\mu}{M}\alpha^2$ terms and thus, the method of calculation can be used for the 2 ^{3}S state.

Table 5.29: Ground State Polarizability Comparison

Contribution	Present Work (a_0^3)	Puchalski (a_0^3)
NR He With Mass Polarization	1.383 809 986 4007(6)	1.383 809 986 408(1)
$\frac{1}{c^2}$	–0.000 080 359 7(3)	–0.000 080 359 9(1)
$\frac{1}{Mc^2}$	–0.000 000 093 5(2)	–0.000 000 093 5(1)

The next table shows a comparison between our calculation of the 2 ^{3}S polarizability with Zhang's calculation [7]. Here, the difference in accuracy between using Hylleraas wave functions with a perturbed Schrödinger Hamiltonian and using CI wave functions with the Dirac equation is apparent. The full relativistic polarizability using the former method is over 4 orders of magnitude more accurate when it comes to convergence accuracy. Furthermore, our calculations include relativistic finite mass effects. This is because there is no rigorously correct way to separate the centre-of-mass motion from the Dirac equation. Since each part of the atom runs on its own clock, there is no centre-of-mass, but only a centre-of-momentum. The mass polarization in the work done by Zhang is a nonrelativistic approximation. This is also why their calculation does not contain the Stone 2 term from Eq.(A.7) in the appendix, a term that arises from switching the Breit interaction from the laboratory frame to the centre of mass frame, similar to mass polarization term in the nonrelativistic Hamiltonian. The faster convergence and the ability to include relativistic finite mass effects are the two main reasons why using the Schrödinger Hamiltonian with Hylleraas wave functions provides a rigorously correct starting point rather than than using CI with the Dirac Equation when it comes to computing the polarizability, and hence the 413 nm tune-out wavelength of the 2 ^{3}S state of helium.

Table 5.30: 2 ^{3}S Polarizability Comparison

Contribution	Our Result (a_0^3)	Zhang et. al. Result [7] (a_0^3)
NR (inf. mass)	315.631 472 376 5(2)	315.631 5(2)
NR (finite mass)	0.188 877 570 3(3)	0.188 9(3)
Relativistic ($m = 0$)	–0.104 253 44(3)	–0.103 9(3)
Relativistic Finite Mass($m = 0$)	–0.000 017 84(3)	
Relativistic ($m = \pm 1$)	–0.095 967 12(3)	–0.095 6(3)
Relativistic Finite Mass($m = \pm 1$)	0.000 010 70(3)	
Stone 2	–0.000 075 659 571(1)	
Total ($m = 0$)	315.716 002 957(11)	315.716 5(4)
Total ($m = \pm 1$)	315.724 296 422(11)	315.724 8(4)

Table 5.31 shows the comparison between the 413 nm tune-out wavelengths. Our final results with all of the perturbations included for the $m = 0$ and $m = \pm 1$ cases have converged to ± 0.00000011 nm, making them more accurate than the results of Zhang et al. [7] by four orders of magnitude for the theoretical tune-out wavelength. However, QED corrections of order α^3 must still be included.

Table 5.31: Tune-out Wavelength Comparison

Contribution	Our Result (nm)	Zhang et. al. Result [7] (nm)
NR (inf. mass)	413.038 304 399(3)	413.0382 8(3)
NR (finite mass)	0.100 917 093(7)	0.100 91(5)
Total Relativistic ($m = 0$)	–0.059 262 97(11)	–0.059 09(4)
Relativistic Finite Mass ($m = 0$)	–0.000 050 745(43)	
Total Relativistic ($m = \pm 1$)	–0.053 396 24(12)	–0.053 29(4)
Relativistic Finite Mass ($m = \pm 1$)	–0.000 045 168(43)	
Total ($m = 0$)	413.079 958 5(4)	413.080 1(4)
Total ($m = \pm 1$)	413.085 825 2(4)	413.085 9(4)

It is shown in Table 5.32 that the difference between the full relativistic tune-out wavelength of order $\alpha^2 \frac{\mu}{M}$ and experiment is about 0.014 nm for the $m = 0$ substate and 0.008 nm for the $m = \pm 1$ substates. This discrepancy is due to QED corrections of the order α^3 [7]. Taking the ratio between the QED corrections and the full polarizability including terms of the order $\alpha^2 \frac{\mu}{M}$ for the ground state from Puchalski's work [18], an estimate can be made for the size of the QED correction to the 2 ^{3}S to 3 ^{3}P transition tune-out wavelength. This estimate is 0.00915 nm making the tune-out wavelength for the $m = 1$ substate with QED included about 413.0949 nm, which differs from experiment by only 0.0011 nm. This agreement warrants the calculation of the QED corrections to the tune-out wavelength. Future calculation of these corrections will allow QED to be tested.

Table 5.32: Comparison with Experiment

Result	Tune-out Wavelength (nm)
$m = 0$	$413.079\,958\,5(4)$
$m = \pm 1$	$413.085\,825\,2(4)$
Experiment	$413.093\,8(9_{\mathrm{stat}})(20_{\mathrm{syst}})$

Chapter 6

Conclusion

By incorporating all contributions to the dynamic polarizability up to the order $\frac{1}{c^2}$ using a perturbed Schrödinger Hamiltonian with Hylleraas wave functions, we were able to compute the most accurate value for the tune-out wavelength of helium closest to the 2 ^{3}S to 3 ^{3}P transition. For the $m = 0$ substate, it is 413.079 958 5(4) nm and for the $m = \pm 1$ substates, it is 413.085 825 2(4) nm. The discrepancy between our calculations and the experiment value of $413.093\,8(9_{\text{stat}})(20_{\text{syst}})$ is about 0.008 nm, which is of the same order of magnitude as the 0.009 15 nm QED approximation. This leads to future, more detailed calculations of the QED corrections to the tune-out wavelength, for the purpose of testing QED. If that calculation is close to experimental value, then this agreement between experiment and theory is a test of QED as an off-diagonal perturbation, rather than a diagonal expectation value. However, if they differ outside of uncertainty, then this opens the possibility of new physics beyond QED.

Chapter 7

Future Work

There is plenty of work to be done regarding the polarizabilities and tune-out wavelengths of atoms. First off, the calculation only included ^{3}S and ^{3}P intermediate states and did not include any D states. This is because the only operator in Eq.(3.28) that connects a S state to the D state to form a nonzero expectation value is the spin-spin operator H_{SS}. Since the contribution to the spin-spin part of the static polarizability from the P states account for 80% of the full spin-spin polarizability [20], the P states were sufficient enough to obtain results that are still well within experimental uncertainty, though the inclusion of the D states will improve the accuracy of the result.
In addition to computing the dipole polarizability, the higher order polarizabilities such as the quadrupole and octopole polarizabilities can be calculated. The higher order polarizabilities can be calculated using the general multipole polarizability formula

$$\alpha_l = -2e\langle\psi^0|r^l C_l^m(\vec{r})|\psi^1\rangle \tag{7.1}$$

[21]

which comes from the multipole expansion of the potential due to the external static field. This equation bears resemblance to Eq.(3.8) because Eq.(3.8) is a special case of Eq.(7.1) where $l = 1$. Calculation of the higher order polarizabilities will allow for

more accurate calculations of the tune-out wavelength.

The higher order terms in the multipole expansion of an oscillating external field must be included as well in order to further increase the accuracy of the polarizability calculation and thus, the tune-out wavelength calculation. This is done by expanding the spacial oscillation of the EM plane wave in terms of spherical waves

$$e^{i\vec{k}\cdot\vec{r}} = \sum_l i^l(2l+1)j_l(kr)P_l(\cos\theta) \tag{7.2}$$

[21]

where $j_l(kr)$ is a spherical Bessel function. These higher order terms describe the change in the electric field over the size of the interacting atom. Currently, no one has included these terms beyond the first order in z. In order to include all of the corrections of order $\frac{v^2}{c^2}$ to the dipole polarizability, the second order term in the expansion must also be included. The multipole expansion of the field however, is not the only type of expansion that will increase the calculation of the tune-out wavelength.

The dipole polarizability itself comes from just one term in the expansion of $\vec{\mu}\cdot\vec{E}$ in terms of field strength F. The constant corresponding to the F^4 term is called the hyperpolarizability [22]. These higher order terms become increasingly important as the electric field strength increases in relevant experiments.

Aside from the implications that the tune-out wavelength and polarizability have on theoretical work, there are also several applications. Using the frequency dependent polarizability, the index of refraction of a gas can be calculated using the formula

$$n(\omega) = 1 + 2\pi N\alpha(\omega) \tag{7.3}$$

where N is the number density and n is the index of refraction [23]. This can be used to determine Avogadro's number N_A. The dynamic polarizability can also be used to calculate the Van der Waals constants [23]. The polarizability also plays a role in atomic clocks. There is a black body shift to the atomic energy levels of the atoms in an atomic clock due to the Stark Effect. This is one of the largest irreducible contributions to the uncertainty of the atomic clock and must be corrected for [24]. Since the black body shift is proportional to the polarizability of the atom [24][25],

this shift can be calculated provided the polarizability is calculated as well.

Most importantly, the tune-out wavelength can be used to test QED. Since the $\frac{1}{c^2}$ ordered contributions are taken care of, what is left are the QED contributions. These contributions are of the order $\frac{1}{c^3}$ and account for interactions with virtual particles in the vacuum. Since these corrections are approximately of the same order as the difference between experiment and theory currently, it is likely that this difference is accounted for by QED.

Appendix

A.1 Brute Force Diagonalization

The pseudospectral solution to the three body Hamiltonian is obtained using a brute force method. First, the Hylleraas functions are orthonormalized by constructing a rotation operator R such that

$$\mathbf{\Phi_m} = R_{nm}\phi_n \tag{A.1}$$

This is done by orthogonalizing the matrix of overlap integrals $O_{mn} = \langle\phi_m|\phi_n\rangle$ with a transformation matrix T such that

$$T^T O T \equiv M = \begin{bmatrix} M_1 & 0 & \dots & 0 \\ 0 & M_2 & 0 & \vdots \\ \vdots & 0 & M_{N-1} & \vdots \\ 0 & \dots & 0 & M_N \end{bmatrix} \tag{A.2}$$

where the only nonzero elements are the diagonal ones.

Then a change of scale matrix

$$S = \begin{bmatrix} M_1^{-1/2} & 0 & \dots & 0 \\ 0 & M_2^{-1/2} & 0 & \vdots \\ \vdots & 0 & M_{N-1}^{-1/2} & \vdots \\ 0 & \dots & 0 & M_N^{-1/2} \end{bmatrix} = S^T \tag{A.3}$$

is applied to M in order to obtain the identity matrix.

$$S^T M S = S^T T^T O T S = 1 \tag{A.4}$$

where $R \equiv TS$. Now that the rotation matrix R which orthonormalizes the wave functions has been obtained, it can be applied to the Hamiltonian to find solutions. This is done by first applying R to the Hamiltonian H, and then diagonalizing that rotated Hamiltonian with a new transformation W such that

$$W^T R^T H R W = \begin{bmatrix} E_1 & 0 & \dots & 0 \\ 0 & E_2 & 0 & \vdots \\ \vdots & 0 & E_{N-1} & \vdots \\ 0 & \dots & 0 & E_N \end{bmatrix} \tag{A.5}$$

where the E_n's are the pseudospectral eigenvalues of the three body Hamiltonian. The qth eigenvector corresponding to the qth eigenvalue is then

$$\Psi^{(q)} = \sum_{mn} R_{mn} W_{nq} \phi_m \tag{A.6}$$

where the coefficients of the eigenvector are $c_m^{(q)} = \sum_n R_{mn} W_{nq}$ [8].

A.2 Stone Terms

The Stone terms, derived by AP Stone are relativistic recoil corrections to the orbit-orbit and spin-orbit interactions. They are the relativistic analogues to the mass polarization term in the nonrelativistic three body Hamiltonian of finite nuclear mass. To derive the Stone terms, we perform a coordinate transformation to the centre-of-mass frame as was done in Eq.(2.2) and Eq.(2.3).

Substituting the transformed coordinates into the orbit-orbit Hamiltonian H_2 gives the Stone 2 term Δ_2.

$$\begin{aligned} \Delta_2 =& \frac{1}{2} Z\alpha^2 \left(\frac{\mu}{M}\right) \left[\frac{1}{r_2}(\nabla_1 + \nabla_2)\cdot\nabla_1 + \frac{1}{r_1^3}\vec{r}_1 \cdot [\vec{r}_1 \cdot (\nabla_1 + \nabla_2)]\,\nabla_1\right] \\ & + (r_1 \leftrightarrow r_2) \end{aligned} \tag{A.7}$$

[26]

Performing the same substitution into the spin-orbit interaction H_3 gives rise to the Stone 1 term

$$\Delta_1 = Z\alpha^2 \left(\frac{\mu}{M}\right) \left[\frac{1}{r_1^3}(\vec{r}_1 \times \vec{p}_2) \cdot \vec{s}_1 + (r_1 \leftrightarrow r_2)\right] \tag{A.8}$$

[26]

which has the same form as the spin-orbit interaction. For the 2 ^{3}S state, $\Delta_1 = 0$ because the spin-orbit contribution is zero and is thus ignored. The Stone term is then just $H_{\text{Stone}} = \Delta_2$.

References

[1] L. J. LeBlanc and J. H. Thywissen. *Species-specific optical lattices.* Phys. Rev. A, **75**:053612, 2007.

[2] B. M. Henson, R. I. Khakimov, R. G. Dall, K. G. H. Baldwin, Li-Yan Tang, and A. G. Truscott. *Precision Measurement for Metastable Helium Atoms of the 413 nm Tune-Out Wavelength at Which the Atomic Polarizability Vanishes.* Phys. Rev. Lett., **115**:043004, 2015.

[3] G. W. F. Drake. *Springer handbook of atomic, molecular, and optical physics.* Springer Science & Business Media, 2006.

[4] G. W. F. Drake. *Encyclopedia of Applied Physics.* WILEY-VCH, 1998.

[5] H. A. Bethe and E. E. Salpeter. *Quantum Mechanics of One- and Two-Electron Atoms.* Springer US, 2012.

[6] J. Mitroy and Li-Yan Tang. *Tune-out Wavelengths for Metastable Helium.* Phys. Rev. A, **88**:052515, 2013.

[7] Y. H Zhang, L. Y Tang, X. Z Zhang, and T. Y Shi. *Tune-out Wavelength Around 413 nm for the Helium 2^3S_1 State Including Relativistic and Finite-nuclear-mass Corrections.* Phys. Rev. A, **93**:052516, 2016.

[8] G. W. F. Drake. *Notes on Solving the Schrödinger Equation in Hylleraas Coordinates for Heliumlike Atoms*, 2016. http://http://drake.sharcnet.ca/mediawiki/index.php/Theory_Notes.

[9] M. M. Cassar (M. Sc. Thesis). *Variational Calculations for General Three-Body Systems*. University of Windsor, 1998.

[10] J. K. L. MacDonald. *Successive Approximations by the Rayleigh-Ritz Variation Method*. Phys. Rev., **43**, 1933.

[11] A. D. Buckingham and J. A. Pople. *Theoretical Studies of the Kerr Effect I: Deviations from a Linear Polarization Law*. Proc. Phys. Soc. A, **68**(10):905, 1955.

[12] L. Landau. *The Classical Theory of Fields*. Butterworth Heinmann, 1975.

[13] C. G. Darwin. *L. I. The Dynamical Motions of Charged Particles. Philosophical Magazine*, 39(233), 1920.

[14] L.I. Schiff. *Quantum Mechanics*. International Series in Pure and Applied Physics. McGraw-Hill, 1968.

[15] A. P. Stone. *Nuclear and Relativistic Effects in Atomic Spectra*. Proc. Phys. Soc., **77**(3):786, 1961.

[16] K. Pachucki and J. Sapirstein. *Relativistic and QED corrections to the Polarizability of Helium*. Phys. Rev. A, **63**:012504, 2000.

[17] M. S. Safronova, U. I. Safronova, and Charles W. Clark. *Magic Wavelengths, Matrix Elements, Polarizabilities, and Lifetimes of Cs*. Phys. Rev. A, **94**:012505, 2016.

[18] M. Puchalski, K. Piszczatowski, J. Komasa, B.ł Jeziorski, and K. Szalewicz. *Theoretical Determination of the Polarizability Dispersion and the Refractive Index of Helium*. Phys. Rev. A, **93**:032515, 2016.

[19] C. S. Estienne, M. Busuttil, A. Moini, and G. W. F. Drake. *Critical Nuclear Charge for Two-Electron Atoms*. Phys. Rev. Lett., **112**:173001, 2014.

[20] G. W. F. Drake. *Tensor Polarizability of the Helium* 2^3S_1 *State*. Phys. Rev. Lett., **24**, 1970.

[21] D.M. Brink and G.R. Satchler. *Angular Momentum*. Oxford science publications. Clarendon Press, 1993.

[22] M. N. Grasso, Kwong T. Chung, and R. P. Hurst. *Hyperpolarizabilities of* H^-*, He, and* Li^+. Phys. Rev., **167**, 1968.

[23] J. F. Babb, K. Kirby, and H. Sadeghpour. *Proceedings of the Dalgarno Celebratory Symposium*. 2009.

[24] M. S. Safronova, M. G. Kozlov, and C. W. Clark. *Blackbody Radiation Shifts in Optical Atomic Clocks.* IEEE Transactions on Ultrasonics, Ferroelectrics, and Frequency Control, **59**(3), 2012.

[25] W. F. Holmgren, R. Trubko, I. Hromada, and A. D. Cronin. *Measurement of a Wavelength of Light for Which the Energy Shift for an Atom Vanishes.* Phys. Rev. Lett., **109**:243004, 2012.

[26] G. W. F. Drake and Z. C. Yan. *Energies and relativistic corrections for the Rydberg states of helium: Variational results and asymptotic analysis.* Phys. Rev. A, **46**, 1992.

Vita Auctoris

Jacob Manalo was born in the year 1990 in Mississauga, Ontario. In 2009, he graduated from Cawthra Park Secondary School and was enrolled in their Regional Arts Program as a visual arts student. At the end of 2014 he completed his Bachelor of Science in Physics from the University of Windsor. He was then enrolled in the Masters of Science Physics program at the same university in 2015 and hopes to graduate at the end of the summer of 2017.